UNITED STATES DEPARTMENT OF THE INTERIOR

GEOLOGICAL SURVEY

Depositional Environment of the Middle Proterozoic Spokane Formation-Empire Formation Transition Zone, West-Central Montana

By

James W. Whipple

Open-File Report 80-1232
1980

CONTENTS

Page

ILLUSTRATIONS

INTRODUCTION

During late Precambrian time, fine-grained siliciclastic and carbonate sediments were deposited in and around an epicratonic basin presently located over portions of Washington, Idaho, Montana, and southern British Columbia and Alberta, Canada (fig. 1). The basin was relatively shallow and tectonically stable over a long period of time, and accumulated a package of rocks approximately 20 km thick known as the Belt Supergroup (Harrison and others, 1974; Harrison, 1972). This basin of deposition has been termed the Belt basin.

Over the last few years, Harrison (1972) and others (Mudge and others, in press) have correlated the stratigraphy in the basin. This monumental task has provided subsequent workers a firm base for studying more detailed aspects of basin sedimentation. Figure 2 represents present-day interpretation of the stratigraphy in the Belt basin.

Traditionally, the contact between the Spokane Formation and the Empire Formation is placed at the boundary where the dominant color of the section changes from red to green. This has led to some inconsistency in mapping, correlation, and interpretation of these formations; however, the change in dominant color has been recognized basin wide and thus remains a primary criterion used for distinguishing these formations.

A distinct transition from red beds of the Spokane Formation to green beds of the conformably overlying Empire Formation is marked by a zone of alternating red- and green-bed sequences. This zone is referred to here as the transition zone or TZ and comprises the upper unit of the Spokane Formation.

Recognition of the depositional environment of the transition zone will aid in understanding the inconsistencies in mapping, correlation, and interpretation of the two formations. In addition, defining a small portion of Belt basin geometry and sedimentation may find application to other Belt Supergroup formations with similar transitional boundaries.

Within the green-bed sequences of the transition zone numerous stratabound sulfide occurrences have been noted (Harrison, 1974, 1972; Clark, 1971). Some of these occurrences might be considered submarginal mineral deposits and have been the subject of intense study (Harrison and Reynolds, 1979; Collins and Smith, 1977; Trammell, 1975). An understanding of the depositional environment of the transition zone when related to the geochemical and diagenetic environments may improve our knowledge of the genesis of such occurrences.

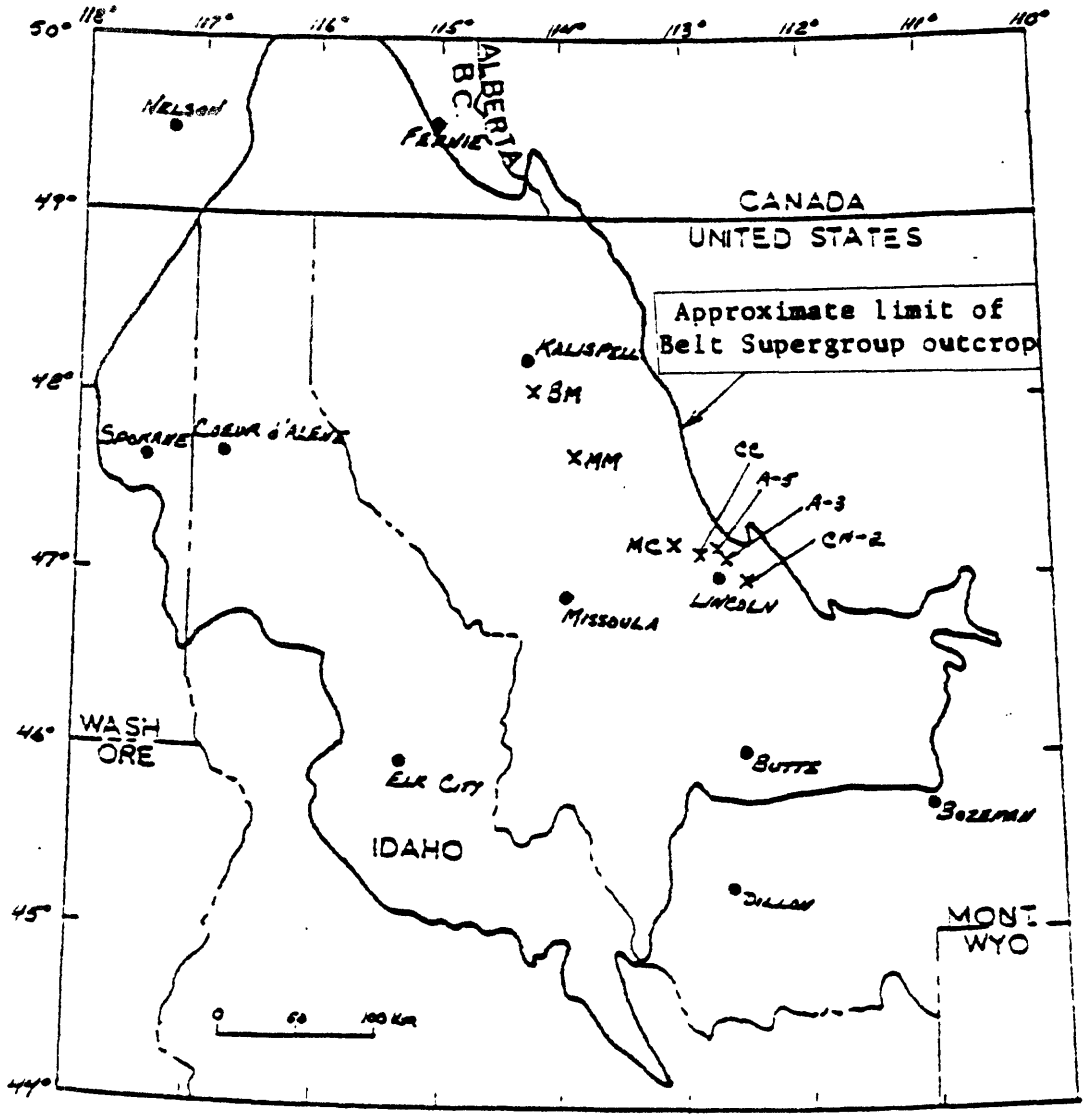

Figure 1.--Generalized location of the Belt basin modified from Harrison (1972, fig. 3). Stratigraphic sections and correlative sections as shown are: BM, Blacktail Mountain Project; CC, Copper Creek; MC, McCabe Creek; MM, Mission Mountains; and A-3, A-5, CH-2, diamond drill holes.

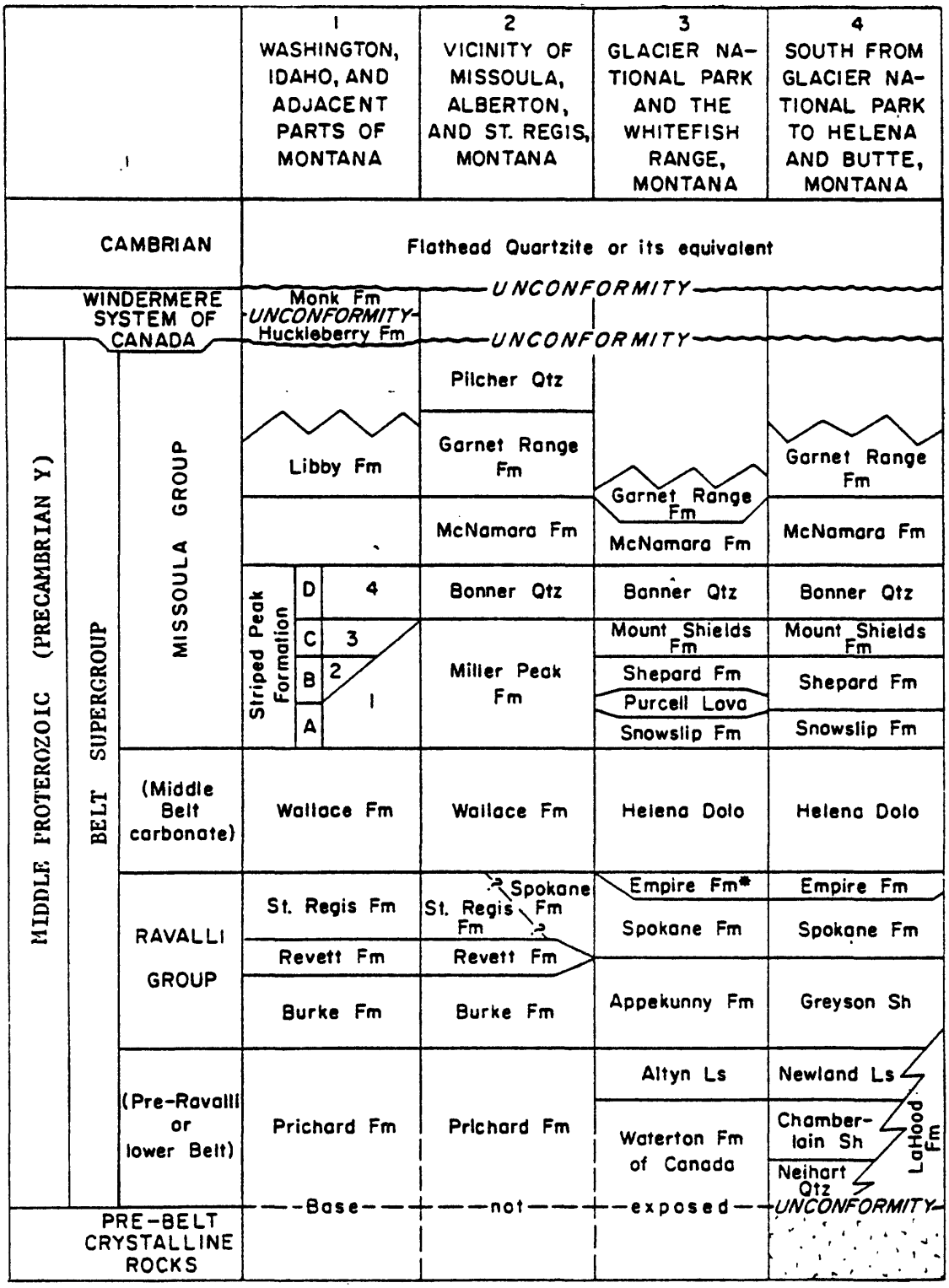

Figure 2.--Present stratigraphic terminology and correlation in the Belt basin, modified from Harrison (1972, fig. 5).

Acknowledgments

I wish to thank my colleagues M. R. Mudge, R. L. Earhart, J. E. Harrison, C. A. Wallace, and M. W. Reynolds for initiating my interest in Belt Supergroup rocks and for their discussion and constructive criticism of the ideas expressed here.

T. R. Walker and D. L. Eicher at the University of Colorado were particularly helpful in reviewing this work, both in the field and in print.

Finally, without the assistance of District Ranger Neil Peterson and his staff of the Lincoln Ranger District, Helena National Forest, many logistical problems could not have been overcome.

Purpose and scope

This study defines the depositional environment of the transition zone through correlation and interpretation of stratigraphic sections prepared from outcrop description and diamond drill hole logs. Two well-exposed stratigraphic sections and three diamond drill holes form the framework for discussion. Outcrop measurement, description, and comparison were accomplished during the summers of 1978 and 1979. Drill-hole information and logs were obtained from Bear Creek Mining Co. during visits to their Spokane, Washington, office and subsequent written correspondence, 1978-1979.

Correlation of the stratigraphic sections provides a means of establishing facies relationships and continuity of red- and green-bed sequences. Interpretation of lithofacies, along with primary sedimentary structures, help in recognition of the depositional environment.

Previous studies

Walcott (1899) named the Spokane Formation and the Empire Formation from exposures in the Spokane Hills and Marysville mining district, respectively, near Helena, Montana. His type localities were incomplete exposures, and the two formations were nowhere described together from the same exposure.

Early mapping and correlation of these formations by geologists quite often lumped the Empire Formation with the overlying carbonate unit (Helena Formation) or the underlying Spokane Formation (Fenton and Fenton, 1937; Ross, 1959, 1963). The Empire Formation was considered a transition zone between the Spokane Formation and the Helena Formation.

More recent workers have recognized the Empire Formation as a separate unit and its transitional relationship to the underlying Spokane Formation. However, the contact between the two formations remains unresolved. In the Big Belt Mountains east of Helena, Montana, Mertie and others (1951, p. 20) concluded that:

> "The contact between the Empire and Spokane shales is gradational and is the most difficult contact in the Belt series to establish and map. At most places it is arbitrarily drawn at the base of the lowest greenish, siliceous shale that characterizes the Empire, but in a few places some of this shale is included in the Spokane."

Klepper and others (1957, p. 6) observed an intertonguing relationship between the Empire Formation and the Spokane Formation in the southern Elkhorn Mountains where they felt that the two were in part at least equivalents.

In other localities, the Empire Formation has not been recognized. Near Evans Peak in the Scapegoat Wilderness northwest of Lincoln, Montana, Mudge and others (1974, p. B11) report that the Helena Formation rests conformably upon the Spokane Formation. At this location there appears to be no Empire strata.

What is the significance of any transition zone if at the localities mentioned above there is no definite Empire Formation? This study attempts to explain these irregularities by examining the transition zone as a time-transgressive series of lithofacies.

Studies concerning the depositional environments of Spokane-Empire sedimentary rocks have been limited and contradictory. Boyce (1973) interprets the Ravalli Group (see fig. 2) as deltaic deposits, whereas Hrabar (1971) sees them as deep-water turbidite sequences. Part of the problem results from interpretation of sedimentary structures and sedimentation sequences and part from correlation of stratigraphic units. Most workers, except Hrabar, agree that Ravalli Group sediments represent a shallow-water environment. An excellent study by Eby (1977) on the middle Belt Supergroup carbonate exemplifies the type of work necessary to interpret depositional environments in Belt rocks.

Geologic Setting

The Belt basin is exposed over an approximate area of 53,000 km^2 as shown in figure 1. Margins of the basin are obscure due to overthrusting and insufficient geologic mapping and interpretation. According to Harrison and others (1974, p. 1), "The Belt basin is one of several epicratonic reentrants formed along the eastern edge of the Cordilleran miogeocline during Precambrian Y time." Other basins he refers to are the Uinta Basin and Apache basin, both reentrants on the North American craton. As cratonic basins, all three are characterized by very thick wedges of shallow water, fine-grained clastic and carbonate sedimentary rocks.

The reported age of the Belt rocks ranges from 1,700 m.y. to 760 m.y. (Obradovich and Peterman, 1968; Harrison, 1972). Ages were calculated by K-Ar and Rb-Sr techniques using whole-rock and mineral samples.

The age of the Spokane Formation has been estimated at 1,300 m.y. (Harrison, 1972, p. 1236). Paleomagnetic studies by Vitorello and Van der Voo (1977) agree well with 1,300 m.y.; however, an age 200 m.y. greater cannot be discounted (Evans and others, 1975).

In light of the foregoing discussion, the age of the Spokane and Empire Formations could range from around 1,500 m.y. to 1,095±22 m.y. as suggested by Obradovich and Peterman (1968, p. 742). This period corresponds to Proterozoic Y time, and commonly throughout this text, the Spokane Formation will be referred to as Ys and the Empire as Ye.

Facies relationships are subtle but pronounced over wide distances in the Spokane and Empire Formations. Stratigraphic sections for measurement description and correlation were selected to emphasize facies relationships. The study area shown in figure 1 indicates the position of these sections.

Source areas for sedimentation during Spokane-Empire time were Belt island to the southwest (Harrison and others, 1974) and cratonic shield areas to the east and northeast (Price, 1964). Because of observed facies relationships and the geometry of the basin, sedimentation within the study area appears to have been from an eastern source.

Belt Supergroup rocks along the eastern limit of the basin are remarkably unmetamorphosed for Precambrian rocks, except locally near intrusives of Precambrian Y and Z, Cretaceous, and Tertiary age. Effects from burial and subsequent regional metamorphism indicate an increase in grade from east to west across the basin (Maxwell and Hower, 1967).

Especially noteworthy is the striking color change in red and to some extent green strata of the Spokane Formation as they become increasingly metamorphosed. In particular, the bright reds and maroons of eastern marginal deposits progressively increase in chroma saturation, approaching grayish-black near intrusive contacts. Red sedimentary rocks in the Mission Mountains and Flathead Range to the west take on purple hues as the effects of regional metamorphism increase.

Sills and dikes ranging in composition from gabbro to diorite are commonly found within the Spokane and Empire Formations and have been dated at 750±25 m.y. or Proterozoic Z age (Mudge and others, 1968, p. E11). Other thin sills of meta-andesite have been assigned a Proterozoic Y age (Earhart, 1975). The younger sills are fairly thick and are bounded by well-developed zones of hornfels. For this reason, stratigraphic sections were chosen to void the hornfelsed zone which may extend far from the sills.

Most of the area lies within the Montana disturbed belt (Mudge 1970) which is characterized by numerous thrust and normal faults. Movement along the thrusts is northeastward and estimated to be as much as 70 km in places (Mudge and Earhart, in press). As a result, several of the stratigraphic sections, if not all, are allochthonous. In this study, all sections were observed in the westernmost thrust plate.

Within the western plate, many sections are offset by west-dipping, listric normal faults. The amount of vertical offset is often small and can be identified.

The net effect of all structures does not negate interpretations on depositional environment if one recognizes that the environment has simply been telescoped eastward. Palinspastic reconstruction awaits detailed stratigraphic studies by workers in other parts of the basin.

Stratigraphic Subdivision

Five stratigraphic sections were chosen for this study. Two sections were compiled from detailed measurement and description of outcrop exposure, and three were constructed from diamond drill hole logs provided by Bear Creek

Mining Company. Locations of the five sections were selected using two criteria:

(1) Best exposure of the transition zone along the eastern limit of the Belt basin.

(2) Increasing offshore distribution to highlight facies changes.

In addition, partial sections were visited in the Mission Mountains west of the measured sections, and drill core penetrating the TZ from the USGS Blacktail Mountain research project even further west was examined at the core library in Denver. Figure 1 depicts the location of the sections relative to the Belt basin.

Rock coloration plays an important role in distinguishing the Ys/Ye contact and limits of the transition zone. Consequently, measurement of the sections began some distance below the lowest green-bed sequence in the upper Spokane Formation and proceeded upward 20-25 m above the highest major red-bed sequence and well into the Empire Formation. The section can thus be subdivided into the upper middle Spokane Formation, the transition zone (upper Spokane Formation), and the lower Empire Formation. Such a scheme would allow correlation of red- and green-bed sequences and provide an interval where lithofacies could be identified and correlated. The drill logs were constructed using the same plan.

Lightness of rock coloration or value and hue are primarily a function of grain size, sorting, depositional environment, and temperature during burial or metamorphism. Carbonate content slightly affects both hue and value.

More detailed description of individual units within the measured sections can be found in Appendix B. Diamond drill logs were not as detailed, and only limited description is present in Appendix B. Terminology used for lithologic description is defined in Appendix A.

PRIMARY SEDIMENTARY STRUCTURES

Features observed in sedimentary rocks, which formed at the time of deposition or shortly thereafter, are termed primary sedimentary structures (Pettijohn and Potter, 1964). As defined by Pettijohn and Potter (1964, p. 3) they include,

> ". . . bedding or stratification, especially the external form of the bed and its continuity and uniformity of thickness, the internal structure and organization of the bed, the interfacial or bedding plane hieroglyphs or markings, both on top and on the bottom of the bed, and the structures produced by soft-sediment deformation."

Primary sedimentary structures abound in Belt Supergroup rocks and are well preserved. Without distinct organisms and fossils, however, interpretation of depositional environments of Precambrian sedimentary rocks has been greatly hindered in the past. More recently, laboratory and field studies relating sedimentary structures to depositional environments have inspired some scientists to tackle this aspect of pG strata (Klein, 1970; Singh, 1969; Gavelin and Russell, 1967).

The emphasis of this paper is on description and interpretation of primary sedimentary structures of the Ys/Ye transition zone as they aid in delineating the depositional environment. This is partially accomplished in the following section where dominant structures are defined and described. Other workers are beginning to recognize the significance of sedimentary structures in Belt rocks, as evidenced by papers presented at the Belt Symposium, 1973, Moscow, Idaho, and more recently by student theses (Bowden, 1977).

Bedding and Lamination

Bedding and lamination thickness determination and terminology are defined in Appendix A.

Graded Lamination

Normal or regular graded lamination consists of sediment grains grading upward from coarse to fine in a single laminae. Bounding contacts between laminae are generally erosional and slightly irregular. Within a graded laminae, sharply defined internal boundaries may exist due to separate mechanisms of sediment transport or sediment load and produce a fining-upward couplet which may appear as two separate laminae.

Graded lamination is common in all sections studied. Lamination consists of couplets that range in thickness from 10 mm to 40 mm (fig. 3). In keeping with the overall trend of the TZ to become finer grained upwards, couplets decrease in grain size upward; that is, fine to very fine grained sand grading to medium silt at the base of the section progressively becomes a couplet of medium silt grading to clay-sized sediment at the top of the TZ. In addition, the coarse-size fraction of the couplet becomes thinner upward, being dominated by clay-sized sediment.

The coarse-size fraction of many couplets is often rippled, indicating traction transport, while the finer grained part of the couplet is draped over the ripples, suggesting suspension sedimentation. Silt and clay couplets may be all suspension sedimentation. Tops of couplets are almost always eroded by the next succession which results in sharp contacts between couplets (fig. 4). Graded couplets in red-bed sequences, although not dominant, exhibit more even and parallel boundaries than green-bed sequences where graded lamination is wavy and irregular (figs. 5, 10).

In outcrop, top set can be determined by superposition of erosional contacts, grain size, and differences in color between the coarse and fine fractions of the couplet. Specifically, in unmetamorphosed red-bed sequences the coarse fraction is lighter in chroma than the fine fraction, whereas in green beds the reverse is true, compare figures 3 and 5.

Graded bedding and lamination is commonly associated with turbidity currents and deep-water sedimentation. These sedimentation units are frequently thick sequences measured in terms of meters. No attempt is made here to elaborate on the various orgins of graded bedding or lamination which are adequately discussed by Klein (1965). However, thin-graded laminations characterize shallow-water deposits, especially in tidal environments of waning current activity (Reineck and Singh, 1975) or waning tidal cycle (Thompson, 1968).

Figure 3.--Graded lamination occurring as fining-upward couplets in red beds. Darker laminae are argillite.

Figure 5.--Graded wavy lamination in green beds, light laminae are fine-grained siltite and argillite. Outcrop wetted to enhance lamination.

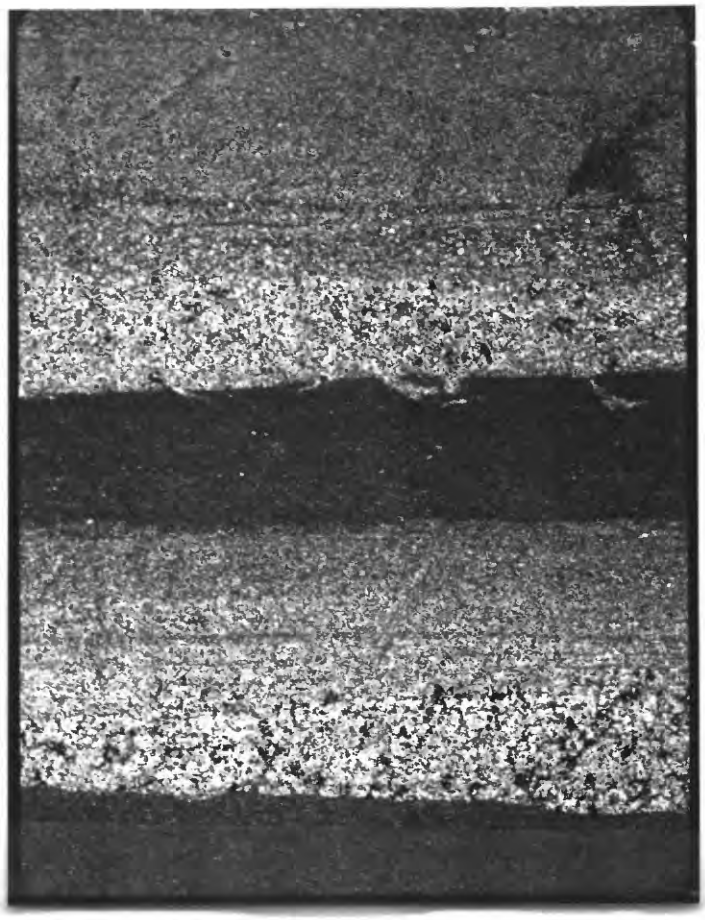

Figure 4.--Thin section of graded lamination in green beds, 10x, partially crossed polars. Note erosional contact between couplets. Black interstitial fillings are copper sulfides.

All graded couplets in the TZ are on a millimeter scale. Hrabar (1973) interprets similar graded sequences in the St. Regis Formation, a probable Spokane Formation equivalent, (fig. 2), as deep-water structures; however, the association with shallow-water features precludes this interpretation.

Planar Lamination

Planar or even, parallel lamination usually consists of very thin laminations, sometimes alternating in color and grain size and sometimes not. Individual laminae or groups of laminae can occasionally be traced or correlated laterally over tens of meters.

Thin planar laminated units as much as 20 cm thick occur infrequently within the TZ. Laminae are less than 5 mm, displaying light- and dark-purple banding and usually within subfeldspathic arenite sedimentation units (fig. 6). Although the lamination type is consistent laterally across the exposure, attempts at correlating laminae for more than 2 m were unsuccessful.

In thin section, dark laminae contain concentrations of elongated mudflakes which are larger than and interspersed among the fabric grains, consisting predominantly of quartz (fig. 7). Hematite, associated with the alteration of clay minerals comprising the mudflakes, produces the darker red coloration. Light-purplish-gray laminae consist of equigranular quartz and feldspar with smaller isolated mudflakes. No apparent difference in size or composition of fabric grains exists between bands.

The larger mudflakes in dark laminae suggest textural grading; however, due to their greater hydraulic equivalence, they were probably transported with the smaller, more-rounded quartz grains and deposited contemporaneously from suspension. That the darker laminae contain an admixture of quartz and mudflakes, while the lighter bands do not, suggests two separate periods of suspension transport and sedimentation.

Textural grading of planar-laminated sediments, such as seen in beach deposits (Clifton, 1969) or turbidite sequences (Kuenen, 1966), was not observed; however, very well sorted beach sand may not show textural grading. Clifton (1969, p. 553) states that regular, nearly parallel lamination of beach foreshore deposits is defined either by alternating layers of different grain size, different heavy-mineral content, or both, whereas the shoreline swash zone is characterized by heavy-mineral lamination and probably typifies the wave or current action necessary for mineralogical grading (Clifton and others, 1971). Heavy-mineral concentrations were not observed.

Planar lamination formed in the upper-flow regime of fluvial environments is often faint and characterized by parting or current lineation (Harms and others, 1975, p. 49). None of the planar laminated units in the transition zone display parting lineation.

Longitudinal bars on the Gum Hollow fan delta of Texas are characterized by parallel lamination always accentuated by ". . . clay pellets, shell debris, or heavy minerals." (McGowen, 1970, p. 43). These bars are low lying, featureless, and confined to the subaerial part of the fan delta termed the fan plain (McGowen, 1970, p. 23).

Figure 6.--Planar laminated, red, subfeldspathic arenite.

Figure 7.--Thin section of arenite shown in figure 6 showing concentrations of mudchips stained by hematite (dark grains), 10x, partially crossed polars. Note slight textural grading.

Suspension clouds in pertidal environments are responsible for evenly laminated sands and silts, especially during storms or by shoaling waves (Reineck and Singh, 1972). In a similar fashion, diurnal tides create small suspension clouds where each tidal stage is characterized by its suspension sediment. Successive tides during a tidal cycle produce a fining-upward laminated sediment resembling graded and planar lamination (Thompson, 1968, p. 36).

Rhythmic Sand And Mud Bedding

Alternating laminae or beds of rippled sand and mud drapes or "flasers" produce a variety of bedding and lamination types often categorized as flaser and lenticular bedding (Reineck and Wunderlich, 1968). The development and preservation of any one variety depends on the intensity of traction or suspension sedimentation. A vertical succession of these sediments produces rhythmic sand-mud bedding (Reineck and Singh, 1975, p. 102), a term that describes the related occurrence of all varieties.

A paucity of sand-sized material results in fewer rippled laminae or beds in the stratigraphic sections. Flaser bedding and lamination are most common in red-bed units toward the top of the transition zone (fig. 8). Here, symmetrical and asymmetrical ripples of subfeldspathic arenite are completely draped by dark-red argillites.

At McCabe Creek, lenticular bedding was observed with flaser bedding in red-bed successions (fig. 9). Most sand lenses still retain a ripple form, although internal structure in the ripple is not discernible in outcrop. According to Reineck and Singh (1975, p. 101),

> ". . . the origin of flaser and lenticular bedding requires conditions of current or wave action depositing sand, alternating with slack water conditions when mud is deposited."

These conditions are commonly found in tidal environments, primarily intertidal zones (Reineck, 1967).

Wavy Lamination

Wavy lamination is described by Reineck and Wunderlich (1968, p. 101-102) and is composed of fining upward couplets of sand or silt and mud. Bounding surfaces between couplets are erosional, with thicker mud laminae distinguishing wavy from flaser lamination.

Couplets of wavy, parallel laminae characterize green-bed sequences and consist of a basal unit of very fine sand or coarse silt, commonly internally cross laminated, draped by silty muds (fig. 10). Upper bounding surfaces of muds show local scouring and filling by the successive coarse fraction. Couplets range in thickness from 3 mm to 10 mm.

Figure 8.--Rhythmic sand-to-mud bedding with well-preserved flasers at top.

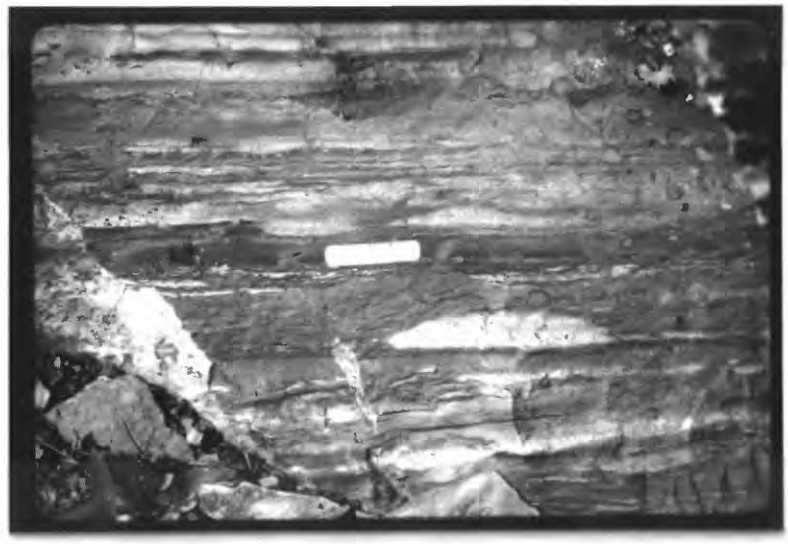

Figure 9.--Lenticular bedding and lamination, light-colored lenses are very fine grained sand.

Figure 10.--Typical wavy, even, parallel lamination of green beds. Slabbed core from Blacktail Mountain.

Preservation of mud laminae in wavy laminated sediment requires low-current velocities, such as recorded in peritidal environments and, in particular, subtidal zones at depths of 4 m to 10 m without appreciable wave action (Terwindt and Breusers, 1972). For example, see Thompson (1968, p. 51, pl. 16) and Reineck (1975, p. 6, fig. 1-1.)

Ripple Bedding and Lamination

Closely associated with flaser and lenticular bedding is ripple bedding in which migrating asymmetrical ripples are developed without well-developed "flasers" (Reineck, 1967; Reineck and Singh, 1975). Included in this category is ripple lamination, either in-phase or in-drift, which occurs when abundant sediment is continually available to currents or waves of lower velocity such that overlapping ripples are formed (McKee, 1965). With the increase in fines to the sediment load, sinusoidal ripple lamination can occur (Jopling and Walker, 1968).

Ripple bedding without mud drapes is rare in the measured sections. One such occurrence was observed in a green-bed sequence (unit 86) of the Copper Creek section (fig. 11). It is small scale, and a set of cross-laminae is less than 3 cm. The ripple bedding is enhanced in outcrop by weathering of carbonate cements in the coarse fraction of the foresets.

Within the transition zone of the Copper Creek section, ripple lamination was observed in one red unit which closely resembles vertically stacked, symmetrical ripples (fig. 12). Some mud is preserved as argillite in the troughs of the ripples and to some extent on the crests. This type of climbing ripple lamination has been termed ripple laminae in-phase (McKee, 1965) and, specifically, sinusoidal ripple lamination (Jopling and Walker, 1968).

Small-scale ripple bedding is found in almost any environment where the bulk of the sediment is noncohesive, sediment supply is low or high, and sediment is actively reworked (Reineck and Singh, 1975). It is most abundant on intertidal sand flats (Reineck, 1967).

Environments that are characterized by the occasional rapid accumulation of sediment are favorable for the formation of climbing ripple lamination. Flood waters of fluvial systems frequently form climbing ripple lamination in overbank deposits where flow is low and sediment accumulation rapid (Harms and others, 1975). Sinusoidal ripple lamination, described by Jopling and Walker (1968), occurs in a Pleistocene kame delta in Massachusetts deposited by sediment-laden melt waters.

Very similar features illustrated and described from the North Sea intertidal flats (Reineck, 1967, p. 196, fig. 11; Singh, 1969, p. 19, fig. 27) have been related to flaser and lenticular bedding and are not necessarily the result of rapid sedimentation.

Figure 11.--Ripple lamination in green calcareous siltite.

Figure 12.--Sinusoidal ripple lamination in red, subfeldspathic arenites with argillite well-preserved in ripple troughs and on some crests.

Algal Lamination and Loferites

Filimentous blue-green algae sustain a variety of growth forms as a reflection of the sedimentary environment. When these forms are preserved in the stratigraphic record they appear as unique lamination types, usually in carbonate sediments. Sediment is trapped and bound by the algae's sticky surfaces, and vertical stacking of sediment and algae layers produces cryptalgal lamination. The term stromatolite has often been used to describe these laminated structures.

Commonly associated with algal lamination of the mat type are void structures, typically alined along bedding planes and collectively called birdseye structures. The laminated calcareous sediments displaying these structures on a millimeter scale are termed loferites (Fischer, 1975).

Cryptalgal lamination was observed only in the Copper Creek section and only in the upper calcareous green-bed sequences of the transition zone (units 53, 55, 57, 59) and the lower strata of the Empire Formation (unit 15). As seen in figure 13, the lamination consists of undulatory to slightly crinkly laminae generally less than 5 mm thick. Planar voids seen along some lamination are birdseye structures. The lamination is interpreted to be former algal mats. No stromatolite heads were observed. Interbedded with the mat-type lamination are mudchip breccias composed of broken and rearranged algal and siltite laminae fragments.

An oncolite, measuring 14 cm long by 7 cm high, was observed in unit 11 of the lower Empire Formation at Copper Creek in association with loferites (fig. 14). The oncolite is truncated at the base, while overlying laminae drape the structure.

Stromatolites have been recognized as intertidal and supratidal environmental indicators (Logan and others, 1964; Logan and others, 1974). However, blue-green algae have been frequently recognized in subtidal environments as well (Gebelein, 1969; Playford and Cockbain, 1969; Hoffman, 1974). They flourish in waters ranging from hypersaline (Logan, 1961) to normal marine.

Oncolites described from recent environments, as well as those described in ancient sequences, are commonly found in subtidal environments (Hoffman, 1974, p. 860; Laporte, 1967; Logan and others, 1964).

Blue-green algae also exist in lake environments (Dean and Eggleston, 1975; Eardley, 1938) and are preserved in the stratigraphic record in such formations as the Green River Formation of Eocene age (Bradley, 1929).

Bedding-Plane Marks and Imprints

Well-preserved primary sedimentary structures found on bedding-plane surfaces provide a third dimension to this study. Most of the marks and imprints are found in the mud layers where parting has preferentially occurred and exposed them on the tops or bottoms of beds.

Figure 13.--Cryptalgal lamination in grayish-green loferites.

Figure 14.--A large oncolite preserved in lower Empire Formation strata. Scale is in millimeters.

Subaerial Shrinkage Cracks

Fine-grained sediments, exposed to the atmosphere, undergo rapid desiccation, resulting in the formation of shrinkage cracks on the exposed surfaces. The network of interconnected cracks forms a characteristic polygonal pattern where the size and shape of individual polygons may vary greatly.

In both measured sections, subaerial shrinkage cracks are abundant in dark-red argillites of the transition zone. The polygons are bounded by 3 to 5 relatively straight cracks intersecting at angles of 70° to 120° (fig. 15). Cracks are generally not more than 5 mm wide and are filled with coarse silt or very fine sand. In cross section they form sinuous, compacted channels normal to the argillite laminae and taper downward, usually terminating near the base of laminae (fig. 16). Associated structures commonly include raindrop impressions, symmetrical ripple marks, wrinkle marks, and probable salt crystal casts.

Few other sedimentary structures are so indicative of their depositional environment as desiccation cracks. An environment which exposes muddy sediment to intermittent wetting and drying often produces rhythmic successions of silt- and sand-filled mudcracks. Numerous fluvial and marine evironments contain subaerial shrinkage cracks. In particular, intertidal zones with extensive mud flats are susceptive to desiccation and cracking after ebb tide and then filling with silt or sand during flood tide.

Subaqueous Shrinkage Cracks

Shrinkage cracks can form subaqueously by the process known as syneresis or the dehydration of clay flocculants (White, 1961). The swelling of clay lattices in response to salinity changes has also produced subaqueous shrinkage cracks (Burst, 1965).

Cracks produced experimentally in the laboratory (White, 1961; Dangeard and others, 1964; Burst, 1965) and those observed and described as subaqueous shrinkage cracks from ancient rocks (Picard, 1966; Donovan and Foster, 1971), all exhibit different crack morphology and occurrence than subaerial cracks. Syneresis cracks are linear, incomplete structures, sometimes oriented but more often not; however, they are almost never connected to form polygons (an exception; Kuenen, 1965).

Within the study area, subaqueous shrinkage cracks were observed exclusively in green argillites of the Copper Creek section, upper TZ, and lower Empire Formation. Cracks occur in two prominent forms; short, linear to arcuate and birdsfeet. The linear forms (fig. 17) are slightly oriented along a NE-SW trend. They are less than 10 cm long and many are arcuate. Fenton and Fenton (1937, p. 1919) best describe birdsfeet cracks in Beltian sediments as ". . . showing radiation of three incomplete cracks from a common center" (fig. 18). Both forms of cracks often display raised relief, and in profile frequently appear as doubly terminated channels (fig. 19). Crack fillings contain both sparry calcite and siltite.

Figure 15.--Subaerial shrinkage cracks forming polygons on a red argillite surface. Cracks are silt-filled and stand in relief to bedding plane.

Figure 16.--Dark lamina in center contains several compacted, subaerial shrinkage cracks as seen in profile. Note the restriction of cracks to the argillite lamina.

Figure 17.--Linear subaqueous shrinkage cracks on a bedding surface in green calcareous siltites of the lower Empire Formation. Note the slight linear trend.

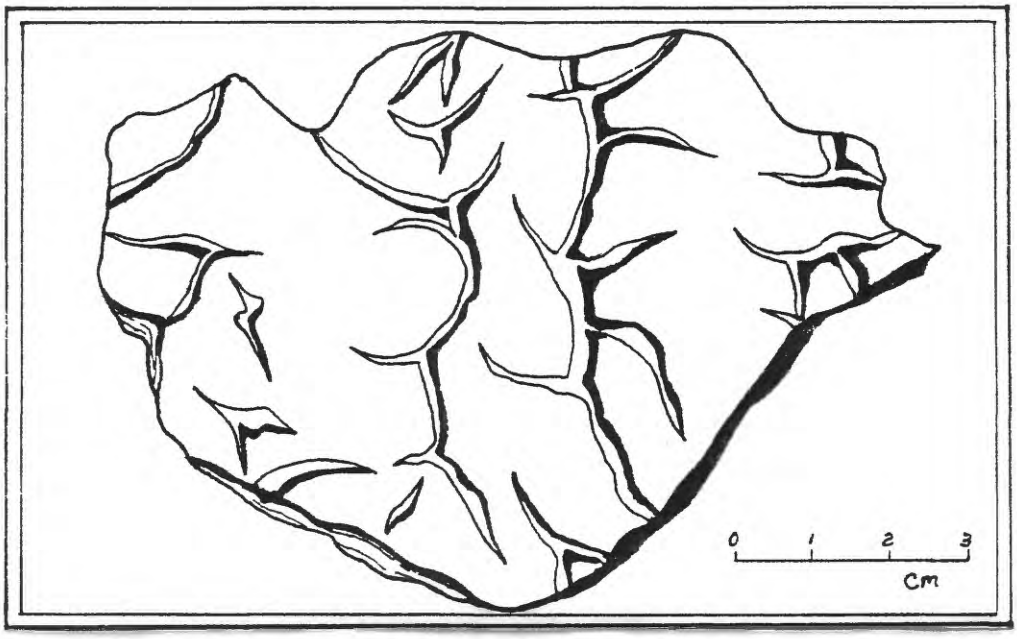

Figure 18.--Birdsfeet subaqueous shrinkage cracks showing incomplete forms and raised relief on bedding-plane surface of argillite.

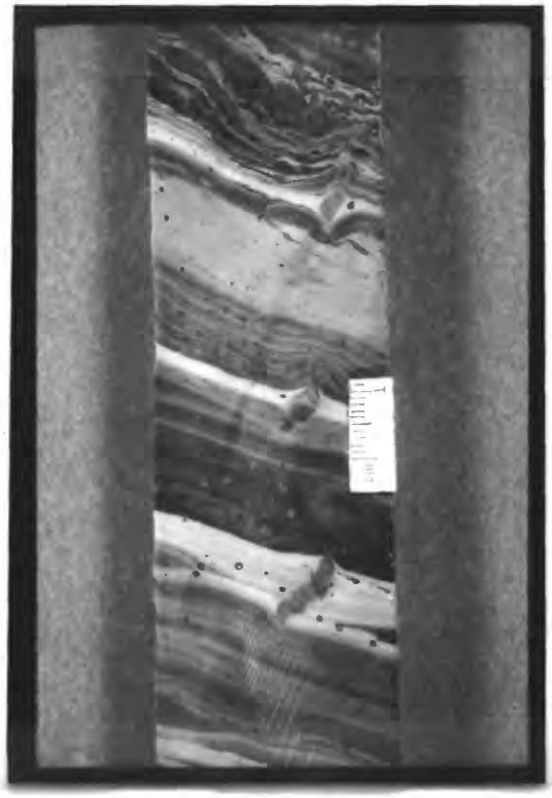

Figure 19.--Subaqueous shrinkage cracks in profile of slabbed green core from Blacktail Mountain. Compacted, doubly terminated cracks in argillite laminae are filled with sparry calcite and siltite.

Bedding-plane surfaces with syneresis cracks do not exhibit any subaerial structures such as raindrop impressions. Associated structures are wavy lamination and gas-expulsion pits.

Although these structures indicate a subaqueous origin, they have been observed in both recent marine and nonmarine environments (Van Straaten, 1954; Picard and High, 1969). In ancient sedimentary rocks, they have been particularly noted in the nonmarine Green River Formation (Picard, 1966) and in the Cathiness Flagstone Series (Middle Devonian) in northeast Scotland (Donovan and Foster, 1972). Donovan and Foster (1972, p. 316) concluded that Cathiness syneresis cracks occurred exclusively in gray-black (N2-N4) and greenish-gray (5GY 6/1) strata and that they formed in quiet waters of lacustrine environments.

Raindrop Impressions

When rain falls on muddy surfaces, small circular impact craters are formed. Elliptical craters occur when the path of the raindrop is oblique to the surface (Shrock, 1948).

Numerous raindrop impressions are found within the TZ red argillite sequences. Elliptical (fig. 20) as well as circular (fig. 21) craters are well displayed on the argillite parting surfaces. Occasionally, impressions are preserved on the crests of oscillation ripples which were drier than the troughs. Spacing of craters suggests that most rainfalls were light and not intense, as overlying and coalescing pits are rare. Craters typically have raised rims on circular shapes, while only the downwind rim of elliptical craters is raised. Note in figure 20 the chatter marks in the bottom of the elliptical craters which are interpreted to have formed from raindrops skidding across the muddy surface.

Raindrop impressions are usually associated with subaerial shrinkage cracks and oscillation ripple marks, suggesting a common environment of intermittently exposed mud flats. Impressions studied by Fenton and Fenton (1937) of Belt Supergroup rocks in Glacier National Park led them to a similar conclusion. When used in conjunction with other structures, Singh (1969) placed them in an intertidal environment for Precambrian rocks of southern Norway.

Gas Expulsion Pits

Circular craters, closely resembling raindrop impressions, form from the escape of entrapped gas in the sediment (Deelman, 1972) or gas produced from decaying organic matter just below the sediment and air or sediment and water interface. In order to rise to the surface, their buoyancy must overcome the weight of overlying sediment and (or) water. Some of these features were termed pit and mound structures by Kindle (1916; 1917).

In a section of lower Empire green beds (unit 11), a bedding-plane surface exposed several circular and slightly elliptical craters, 1-4 mm in diameter, frequently filled with microspar (fig. 22). Concentrically surrounding the pit are small hairline cracks which appear to have been produced by collapse of marginal sediment perhaps into the escape channel (fig. 23). Raised rims are absent. Fluid escape channels are associated with

Figure 20.--Raindrop impressions preserved as elliptical craters on a red argillite surface. Note chatter marks in bottom of craters. Wind blowing from right to left.

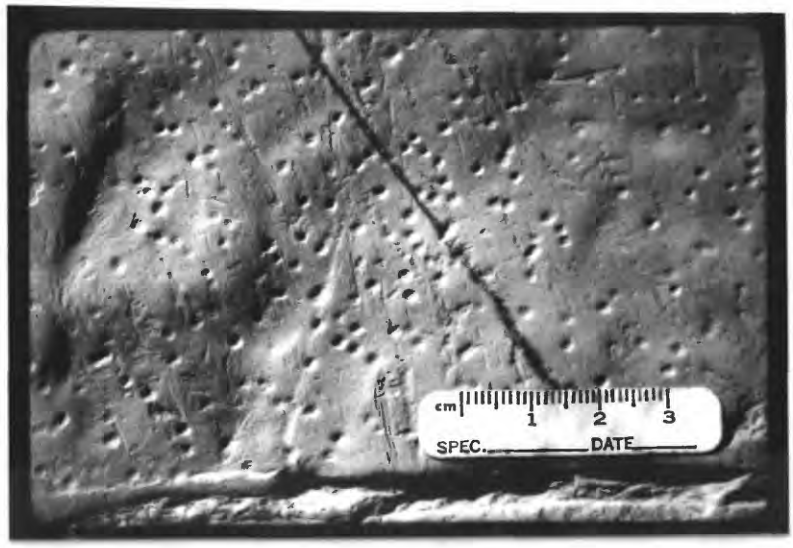

Figure 21.--Bedding-plane surface illustrating circular raindrop impressions. Grooved striations are from recent ice movement over the surface.

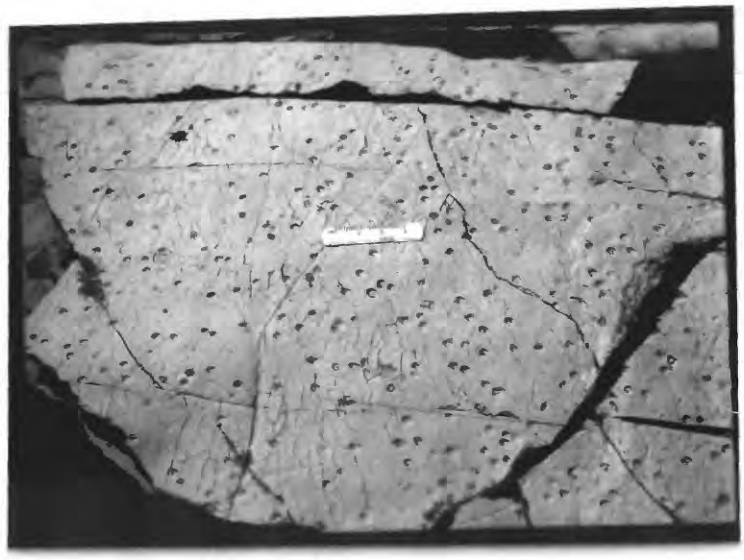

Figure 22.--Gas expulsion pits on bedding plane of green calcareous siltite in the lower Empire Formation. Scale is 3 cm long.

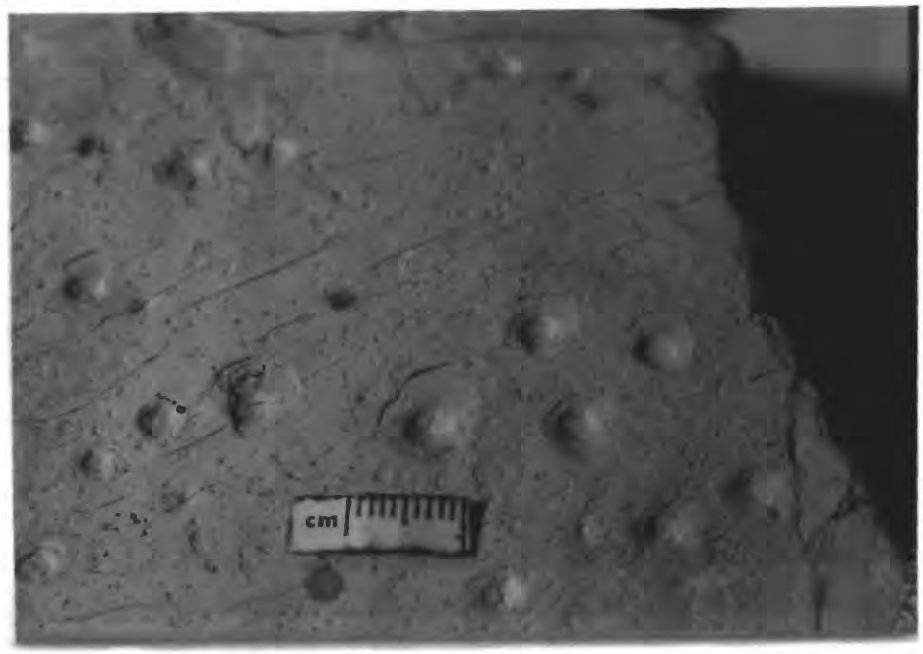

Figure 23.--Closeup of gas expulsion pits showing marginal, concentric cracks to the pit perhaps formed from collapse of pit into escape channel.

the gas expulsion pits, as well as syneresis cracks, birdseye structure, and algal lamination.

Slabs sawn longitudinally through the pits failed to uncover vertical escape channels. It is assumed that the tubes or channels closed after passage of the gas bubbles, similar to that described by Shrock (1948, p. 133).

Spherical gas expulsion pits have been produced experimentally (Shinn, 1968; Deelman, 1972) and described from recent environments (Shrock, 1948; Shinn, 1968; Dunham, 1970). Likewise, craters attributed to gas bubble escape have been described from ancient rocks (Ham, 1952; Illing, 1959) and in Belt rocks by Fenton and Fenton (1937, p. 1924).

Whatever the source of gas, whether organic or entrapped, pits are often found in close association with birdseye structure, in calcareous sediments, and filled with sparry calcite or anhydrite (Deelman, 1972). They can form underwater (Shinn 1968) or through capillary action on rewetted desiccation surfaces (Deelman, 1972). Likely settings to find such structures would include shallow water to intermittently exposed fresh or marine environments.

Salt Crystal Casts

Crystals of halite that form from evaporation of hypersaline waters or precipitated from brines are occasionally preserved as casts filled by sediment and (or) sparry calcite. They are found on bedding-plane surfaces and interstitially in the sediment.

Although common in younger Belt formations, salt casts in the Spokane Formation have rarely been reported (Fenton and Fenton, 1937).

Within the upper part of the Ys/Ye transition zone, one set of surface markings was observed that closely resembles the cornices of salt casts, less than 5 mm in overall size (fig. 24). They are associated with subaerial shrinkage cracks in red argillites.

Salt is precipitated in both subaerial and subaqueous environments, the only common denominator being saturated waters or brines with respect to NaCl. Marine waters and arid climates often produce the right conditions for salt precipitation.

Wrinkle Marks

Wrinkle marks or Runzelmarken are small structures developed on the surface of partly cohesive, fine-grained sediments. Reineck (1969) found experimentally that wrinkle marks form from strong winds blowing over sediment covered by thin films of water (1 cm or less).

These markings were occasionally observed in red-argillite sequences of both sections (fig. 25). The markings were not oriented.

Wrinkle marks are considered a good indicator of intermittently exposed sediment surfaces (Reineck and Singh, 1975, p. 56). Similar structures produced by turbidity currents (Dzulynski and Simpson, 1966) appear to have preferred orientation.

Figure 24.--Probable salt crystal casts in red argillite.

Figure 25.--Wrinkle marks on the surface of red argillite.

Mudchip Breccias

Bedding-plane surfaces, composed entirely of mud or argillite chips, often accompany sediments which are intermittently exposed to desiccation. Polygons of subaerially cracked surfaces are ripped up by wind and water currents upon being rewetted and redeposited as laminates of mudchip breccia. Individual clasts are very thin plates, often deformed, rounded to angular, and varying greatly in size. The term rip-up clasts has been applied to the breccias by many workers.

Mudchip breccias in the study sections are as common, if not more so, than shrinkage cracks, especially in red argillites. Clasts are thin subrounded plates varying in size from 1 mm to 2 cm (fig. 26). Edgewise and imbricated clasts were not observed. Subaerial shrinkage cracks, associated with the breccias, are commonly filled with mudchips.

The association of mudchip breccias and shrinkage cracks in red beds is a good indicator of intermittent exposure and reworking of sediment surfaces. Occasional breccias observed in green strata may represent reworking of sediments by currents in a subaqueous environment, or perhaps they were orginally red sediments.

Target Marks

Conspicuous circular targets of concentrically arranged color bands characterize some bedding-plane surfaces in red beds. They have been observed in the Supai Group in the Grand Canyon, as well as in many other red beds, and are commonly composed of white to tan rings with black to dark-red bands nearer a well-defined center.

In the Copper Creek section, beds of targets were traced laterally for at least 10 m. Individual targets range in size from 2 cm to 10 cm in diameter (fig. 27). Light-pale-green to beige bands form the outer rings, whereas shades of red dominate inner bands. The bullseye is typically dark red or black in color. No disruption of sedimentary textures or fabric is evident around or in the targets, and color banding appears to be the result of differential bleaching. Targets are confined to individual sedimentation units (unit 21, upper middle Ys) commonly as single structures and rarely as coalescing orbs.

There may be some question as to these features being sedimentary structures; certainly, the color banding is secondary, but their confinement to individual sedimentation units appears to be a depositional phenomena. It is likely that bleaching and subsequent color banding is a diagenetic process. Earhart and others (1977) describe such features from the Spokane Formation of the Belt Supergroup and ascribe their origin to the possible radiogenic decay of detrital zircons. Whatever their origin, further study may reveal information on depositional environment provided the source of the targets is related to sedimentation.

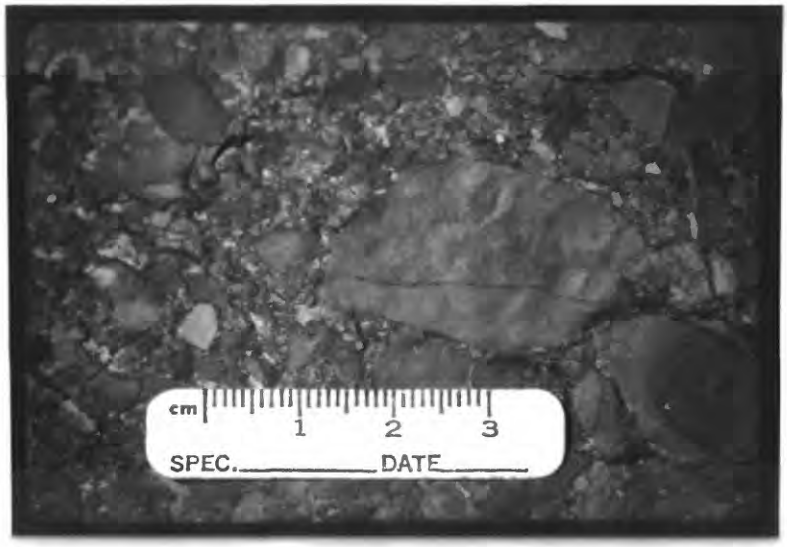

Figure 26.--Top of a mudchip breccia. Note the lack of size sorting.

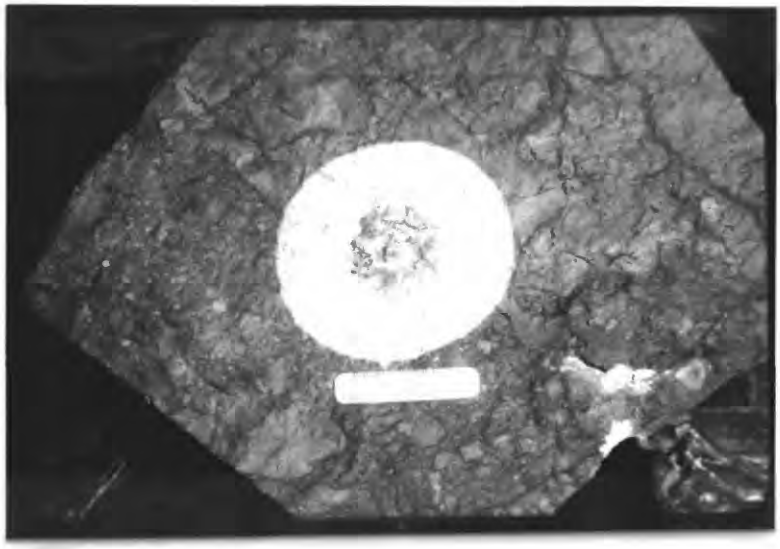

Figure 27.--A typical target mark exposed on a red bedding-plane surface. Outer ring is light grayish green while the center is reddish brown.

Flow Structures

Near linear bedding-plane structures, formed by directional currents and preserved on the lower or upper bed surface, are collectively termed flow structures (Glaessner, 1958). They include scour marks, such as flute and groove casts, as well as flow ridges and obstacle marks. These structures are attributed to strong current action on firm mud bottoms (Kuenen, 1957; Dzulynski and Sanders, 1962; Dzulynski and Simpson, 1966).

Markings closely resembling flute casts were observed on the bottoms(?) of red float in the Copper Creek section, but none were seen in place. These structures, as seen in figures 28 and 29, are not common. They are composed of very fine grained arenite surrounded by argillite, having bulbous heads and tapering tails. No distinct obstacles at the head of the markings were observed, and it is suspected that the original structures were depressions and not ridges.

Regardless of the type of flow structure, it is curious that such markings are found in association with subaerial and shallow-water structures as they are commonly described from deep-water turbidite sequences.

However, experimental production of such structures indicates that two basic requirements are all that are needed; (1) an alternating sequence of argillaceous and arenaceous sediments, and (2) strong currents of varying velocity (Glaessner, 1958, p. 6). Although recognized and characterizing flysch deposits, flute casts and other sole markings have been observed in fluvial-deltaic deposits (Glaessner, 1958; Dott and Howard, 1962), and Potter and Pettijohn (1977) focus on their importance as paleocurrent indicators rather than environmental significance.

Ripple Marks

Ripple marks are particularly well displayed on bedding-plane surfaces, and are probably the most common of primary sedimentary structures. Many varieties have been described and attributed to currents, waves, and winds. Ripples can be classified as asymmetrical or symmetrical without having genetic implications. A useful measurement of ripples called the ripple index (Bucher, 1919), or ratio of crest wavelength to amplitude (Potter and Pettijohn, 1977, p. 115, fig. 4-13), has been used to distinguish both form and origin (Reineck and Singh, 1975).

Dominance of finer grain sizes in the TZ does not lend itself to forming abundant ripples; however, both asymmetrical and symmetrical ripple marks, composed mostly of very fine grained sand and coarse silt, are present in all sections. Asymmetrical ripples are straight crested and most often found in green beds. Ripple indices measured for asymmetrical ripples range from 6.4 to 9.0. Symmetrical ripples are more common in red beds and generally have sinuous crests. Rippled marked bedding planes are not as common as ripple lamination.

Truncated or flat-topped asymmetrical ripples were observed in the Copper Creek section (fig. 30). These ripples were in arenite, exhibiting straight, flattened crests.

Figure 28.--Oriented flow structures on the bottom(?) of a red argillite.

Figure 29.--Closeup of flow structures. Note the absence of obstacles at heads of marks.

Figure 30.--Truncated or flat-topped asymmetrical ripple marks. Note raindrop impressions on flattened crests. Current from left to right.

Ripples are most frequent in shallow-water environments (Blatt and others, 1972, p. 193; Potter and Pettijohn, 1977), but are also present in deep-water sediments. Truncated or flat-topped ripples are formed by falling water during emergence and are an excellent indicator of shallow water (Tanner, 1960). Flat-topped ripples are commonly found in intertidal environments where ebb tides truncate ripples formed during flood tides (Blatt and others, 1972, p. 154).

Deformational Structures

Bedding and lamination, deformed penecontemporaneous with sedimentation, results in a variety of sedimentary structures considered primary and possibly indicative of depositional environment. Local disruptive features produced by slumping, loading, or injection have been termed soft sediment deformational structures, and generally they best illustrate the conditions of sedimentation and the saturation or weight of the sediment. Load casts, ball-and-pillow structures, and soft sediment injection features are described herein.

Load Structures

Sand deposited over hydroplastic muds often founders into the mud layers creating irregular sand pockets. These pockets are preserved on the base of sandstone beds as load casts or seen in profile as sand bulges sagging into mud laminae. Load structures vary in size from several millimeters to several decimeters (Potter and Pettijohn, 1977, p. 198).

Load structures are common in the upper red arenite and argillite sequences of the transition zone at all localities. They are composed of very fine grained subfeldspathic bulges sunk into thin laminae of argillite alternating with arenite (figs. 31, 32). The sand pockets average 3 cm in width and have downwarped underlying and marginal laminae. Most load structures contain mudchips.

Load structures are not indicative of any particular environment (Potter and Pettijohn, 1977). Their formation only requires sand deposition over hydroplastic muds. They are regularly found in flysch deposits and occasionally in some fluvial and intertidal environments where rapid mud sedimentation is interspersed with sand deposition (Reineck and Singh, 1975).

Ball-and-Pillow Structures

Ellipsoidal bodies of sand, appearing on the base of sand strata and within mud layers, are termed ball-and-pillow structures. These features are sometimes internally laminated, grade up into undisturbed sand, and range in size from a few centimeters to a few meters (Potter and Pettijohn, 1977). They have been produced experimentally (Kuenen, 1965), and most workers agree they are the result of water-saturated sand foundering into underlying muds with primarily vertical movement.

Figure 31.--Load structure of subfeldspathic arenite deforming interlaminated argillite. Downwarping of truncated laminae is common.

Figure 32.--Closer view of a load structure. Mudchips are frequently incorporated in the sand pockets.

Ball-and-pillow structures occur frequently in the Copper Creek section and rarely in the McCabe Creek outcrops. They appear as inverted mushrooms of sand 3-10 cm wide, often isolated from arenite beds (figs. 33, 34). The structures most often occur within argillites or siltites and are always encased with an argillite sheath.

All ball-and-pillow structures observed showed internal lamination that is conformable with the shape of the structure. Laminae converge at the upper corners and top of structure but are not truncated. Instead, they expand out into overlying strata. Internal lamination at Copper Creek consists of alternating light- and dark-red laminae, while at McCabe Creek internal laminae are not apparent.

Although ball-and-pillow structures are not unique to any environment, they, like load casts, indicate rapid sedimentation of saturated sand over mud. They have been observed in all types of environments where conditions were favorable. Sorauf (1965, p. 554) cites several examples in ancient rocks which have similar form and possible genesis.

Small-Scale Diapiric Structures

Discordant structures, produced by upward intrusion of soft sediment into overlying strata, have various terminology such as injections or dikes, and are reviewed in Lowe (1975, p. 175-176). Mobilization of soft sediment on a small scale that results in the injection of either fine- or coarse-grained material into overlying, somewhat rigid sediments is considered a process resembling diapirism (Daley, 1971). The force mobilizing sediment upward may be the result of loading, depth of burial, and (or) effective hydrostatic pressure (Swarbrick, 1968). Channelways, cracks, pipes, or other passageways are not necessary as a precursor for intrusion. Thus, intrusion is probably rather forceful, occurring soon after deposition of the sediments.

Small-scale diapiric structures observed in the Copper Creek section are confined to red mud or argillite intrusions. These anticlinal features are approximately 6-10 cm in width and height, penetrating an arenite bed above (fig. 35). Argillite laminae within the structure conform to its shape, closely resembling a cabbage head. The overlying arenite does not truncate the upper surface of the intrusion nor is it obviously deformed by the argillite.

Intrusion of mud by hydroplastic flowage occurs at shallow depths of burial and from locally excessive hydrostatic pressures (Swarbrick, 1968) possibly produced by load consolidation. This type of loading occurs when sediments are deposited at high instantaneous rates in sequences of alternating mud and sand (Lowe, 1975, p. 197). Shallow-water marine, fluvial-deltaic, and deep-sea environments all contain such conditions of sedimentation.

Figure 33.--Ball-and-pillow structure at McCabe Creek. Light-colored sediment is sand. Note absence of well-defined internal lamination.

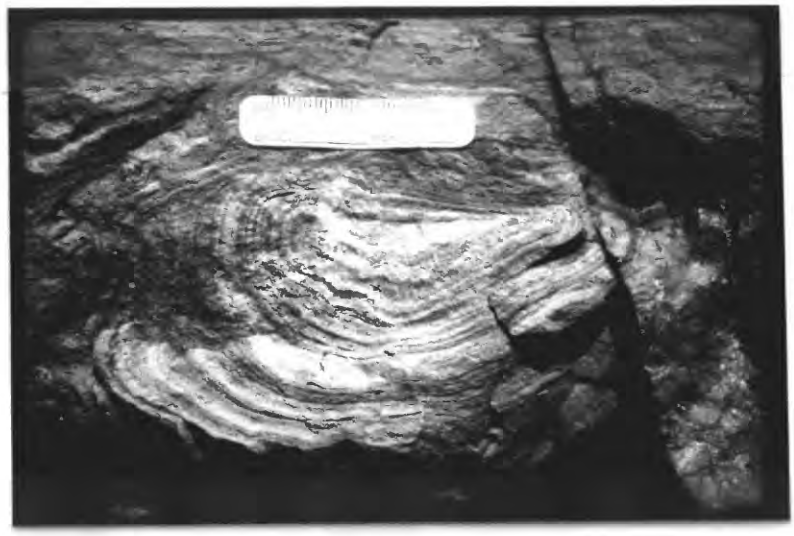

Figure 34.--Typical ball-and-pillow structure at Copper Creek. Internal laminae converging at upper corners is readily apparent.

Figure 35.--Diapiric structures of dark-red argillite penetrating an arenite bed. Truncated arenite and overlying laminae do not show any upwarping.

Fluid-Escape Structures

Consolidation of sediments results in pore fluid expulsion in noncohesive materials where pore fluids, although commonly thought of as water, may include gas. Fluid loss or escape is accomplished by three basic mechanisms: (1) seepage, (2) liquefaction, and (3) fluidization (Lowe, 1975). Primary sedimentary structures associated with fluid escape discussed here are the result of fluidization and include birdseye structures.

Fluidization Channels

Escaping pore fluids that fluidize sediment and generally form discordant structures filled with the sediment are termed fluidization channels (Lowe, 1975, p. 167). These features are often small, but may include a group of structures called clastic dikes (Shrock, 1948).

In both red- and green-bed sequences of the TZ, small-scale fluidization channels commonly penetrate interlaminated arenite and argillite. They appear as discordant, sinuous, sand-filled bodies, typically containing mudchips and terminating downward (figs. 36, 37). Laminae truncated by channels are disrupted and deformed at the margins of the channel. Upper reaches of a channel may spread and disperse horizontally into arenite laminae, sometimes reappearing centimeters away as a renewed channel. On bedding-plane surfaces they closely resemble mudcracks but are more linear and do not form equal polygons. Close association with mudcracks leads one to suspect that some cracks may act as pathways for fluidized sediment.

Lowe (1975, p. 197) concludes that prodeltaic and deep-sea continental rise sediments frequently display fluid-escape structures because of the rhythmic deposition of sediments. Similar features described by Hoffman (1975) as syneresis dikes in lower Proterozoic rocks are ascribed to a shallow-marine environment. Winston (1977) relates fluid-escape structures in younger Belt rocks to sediments on seaward parts of sea marginal flats.

Birdseye Structures

Voids or vugs in calcareous rocks that are filled with calcite resemble birdseye structures. They are isolated bubble or planar shapes, millimeters in dimension, and formed primarily by escape of gas either entrapped in the sediment or produced from organic decay.

Calcareous green siltites of the TZ and lower Empire Formation (Copper Creek section) frequently contain birdseye structures. As seen in outcrop, they occur as planar voids in vertical section, 3-5 mm high by 5-20 mm long, and oriented along lamination (fig. 38). On unweathered surfaces they are filled with calcite. They are associated with typical green bed wavy lamination and to some extent cryptalgal lamination. Individual sedimentation units displaying these structures have good lateral continuity.

Interpretations have been made that birdseye structures are intertidal and supratidal paleoenvironmental indicators (Friedman and Sanders, 1978, p. 334; Shinn, 1968). However, like most sedimentary structures, similar features have been observed in other environments in both carbonate and siliclastic rocks (Deelman, 1972; Laporte, 1967), and Ginsberg (1975, p. 198) suspects that birdseye structures may develop in subtidal sediments.

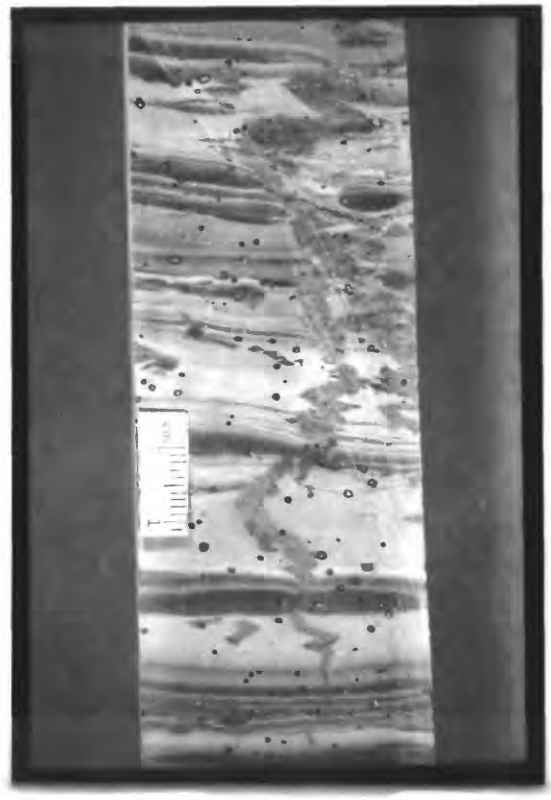

Figure 36.--Fluidization channel in slabbed green core from Blacktail Mountain.

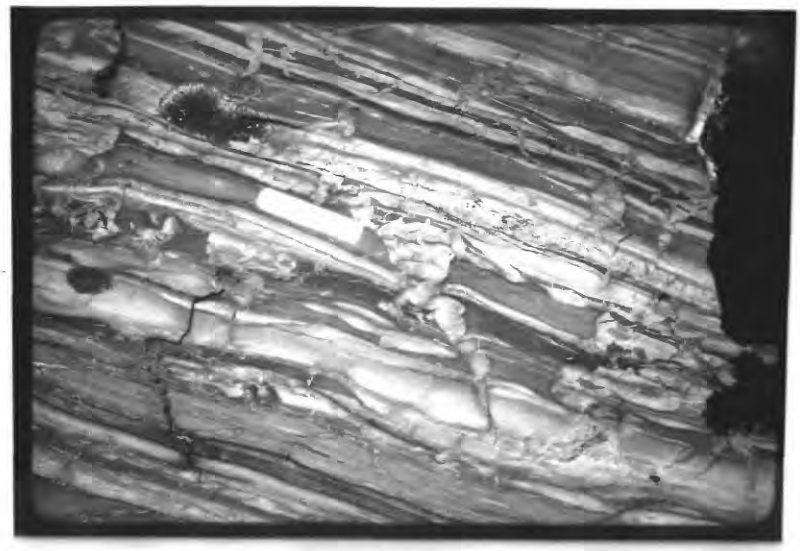

Figure 37.--Similar fluidization channel in red beds at Copper Creek. Channels most often begin and end in arenite laminae.

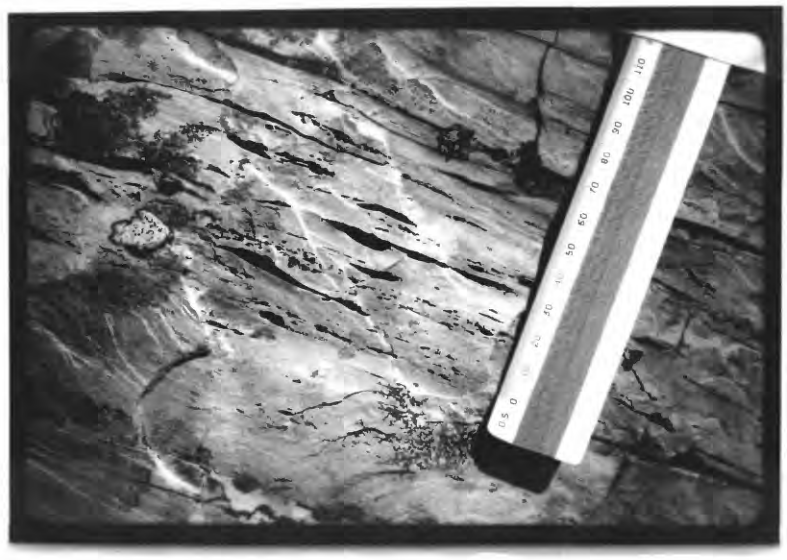

Figure 38.--Birdseye structure in calcareous green siltites from the transition zone. Voids formed from the dissolution of calcite fillings. Scale is in millimeters.

Contorted Structures

Lamination which is deformed into a series of sharp crested anticlines and open synclines is generally termed convolute lamination. The internal folding produces contorted structures that appear primary and the result of either currents or loading or both. In addition, fluid escape during loading and compaction may promote convolution.

Contorted structures observed at Copper Creek consist of small-scale symmetrical anticlines in red calcareous argillites with thin interlaminae of very fine grained arenite. Fluidization channels occupy anticlinal axes (figs. 39, 40) and penetrate surrounding strata. The structures are confined to one sedimentation unit and persist laterally for tens of meters. Undeformed, overlying sediments do not truncate the structures.

Similar convolute laminations in fine-grained sediments are produced mainly by differential loading and dewatering (McKee and Goldberg, 1969, pl. 2). Contorted structures are found in a variety of shallow-water environments (Dzulynski and Smith, 1963; Dott and Howard, 1962), as well as the better known deep-water occurrences. The structures observed in the Ys/Ye transition zone appear to be the result of differential loading and not the result of current action.

LITHOFACIES

The stratigraphic sections, having been subdivided into upper middle Ys, Ys/Ye transition zone, and lower Ye, are herein further subdivided into distinct lithofacies which are dependent on dominant lithology, color, carbonate content, bedding and lamination style, and sedimentary structures. One or more of four basic lithofacies, designated A through D, characterize each of the three stratigraphic subdivisions. Stratigraphic descriptions of drill core from the three holes is limited and does not permit complete lithofacies description comparable to the measured sections.

Lithofacies A

Subfeldspathic arenites are interlaminated with siltites and argillites as fining-upward rhythmic successions as much as 11.5 m thick. A typical succession begins with arenite, often ripple cross-laminated and forming ball-and-pillow structures at its base, especially at Copper Creek. Upward, arenites become interlaminated with siltite which in turn becomes interlaminated with argillite. Argillites that conclude the succession exhibit subaerial shrinkage cracks and mudchip breccias, resulting in discontinuous, even, parallel lamination. All units are red and noncalcareous.

Lithofacies B

Very thin, discontinuous, even, parallel laminated argillites contain occasional thin, lenticular siltite and subfeldspathic arenite laminae. Subaerial shrinkage cracks are often silt filled and, along with mudchip breccias, are more numerous at Copper Creek than McCabe Creek. Thick, gray-green to pale-green laminae of argillite less than 20 mm thick are sparsely present. For the most part this lithofacies remains noncalcareous to slightly calcareous even though enclosing units often contain much carbonate.

Figure 39.--Contorted structure in red argillites of the transition zone.

Figure 40.--Anticlinal contorted stuctures with fluidization channels occupying axes. Note the lack of disruption in overlying argillite laminae.

Lithofacies C

This red, calcareous lithofacies is characterized by rhythmic sand-to-mud bedding mainly as flaser and lenticular lamination. Other types of lamination occasionally present are planar and graded (figs. 3, 6). Flaser lamination consists of rippled subfeldspathic arenite with overlying fine-grained siltite and argillite preserved in ripple troughs and to some extent over crests. Lithofacies C at the top of the transition zone contains thinly bedded arenite with pyrite casts. Thick, intercalated green laminae (20 mm) are sparsely present and discontinuous laterally over tens of meters.

Primary sedimentary structures abound in this facies. Especially prolific are subaerial shrinkage cracks and raindrop impressions in argillite and fluid escape and load structures. Also found are truncated asymmetrical ripple marks, wrinkle marks, diapiric and contorted structures, and flow structures.

Lithofacies D

Green, wavy, parallel laminated calcareous siltites and argillites typify this lithofacies. At Copper Creek, upper green units contain much algal lamination as well. Clean, whitish quartz arenites are commonly interlaminated with siltite and argillite couplets. Within the transition zone, lithofacies D alternates with C in two intervals which can be correlated across the study area (figs. 41, 42).

Subaqueous shrinkage cracks, birdseye structures, gas expulsion pits, and algal lamination are unique to this lithofacies. No subaerial or emergent structures were observed in green beds. Stratabound sulfide minerals are likewise confined to green sequences, although not all green sequences are mineralized. Deformational, contorted, and fluid escape structures are rare. Asymmetrical ripples are confined to quartz arenite laminae and beds.

CORRELATION

Correlation of stratigraphic sections can be accomplished using lithofacies and color. Figures 41 and 42 illustrate the correlation. In particular, the thickness of red and green sequences varies across the study area in response to the geometry of the depositional environment. Lithofacies defined by dominant grain size, rock color, carbonate content, and sedimentary structures correlate well laterally.

Lithofacies coarsen eastward; that is, the sand-size fraction becomes more abundant shoreward. In addition, obvious changes in dominant grain size occur at the top and bottom of the transition zone in both measured sections (figs. 43, 44).

Individual sedimentation units, namely the thicker sand bodies, show a possible correlation between measured sections. Compare units 63, 56, and 29 of the McCabe Creek transition zone with units 79, 74, and 38, respectively, of the Copper Creek section, from description in Appendix B.

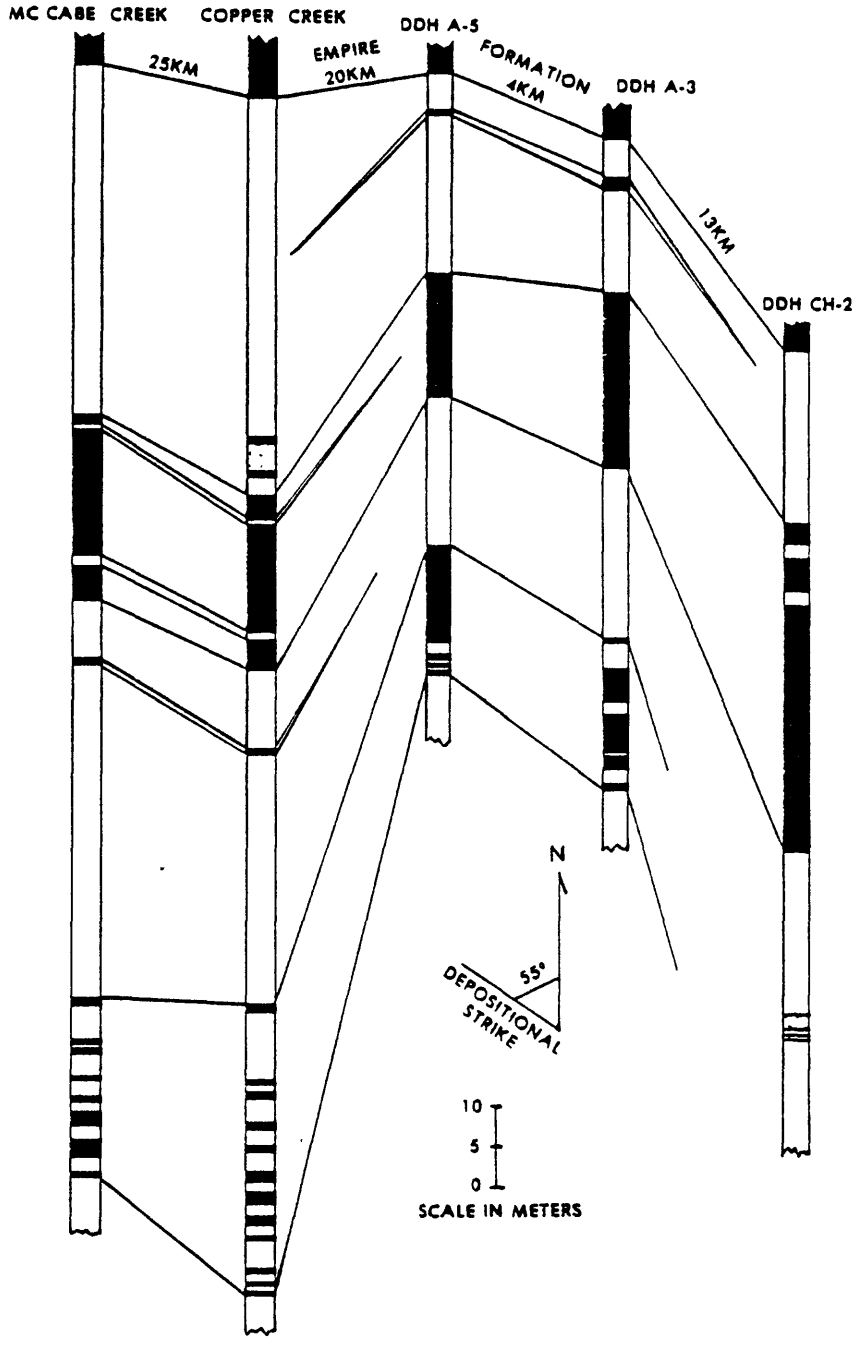

Figure 41.--Correlation of oxidized, red-colored lithofacies (A,B,C) and reduced, green-colored lithofacies (D) within the transition zone. Red, white; green, black.

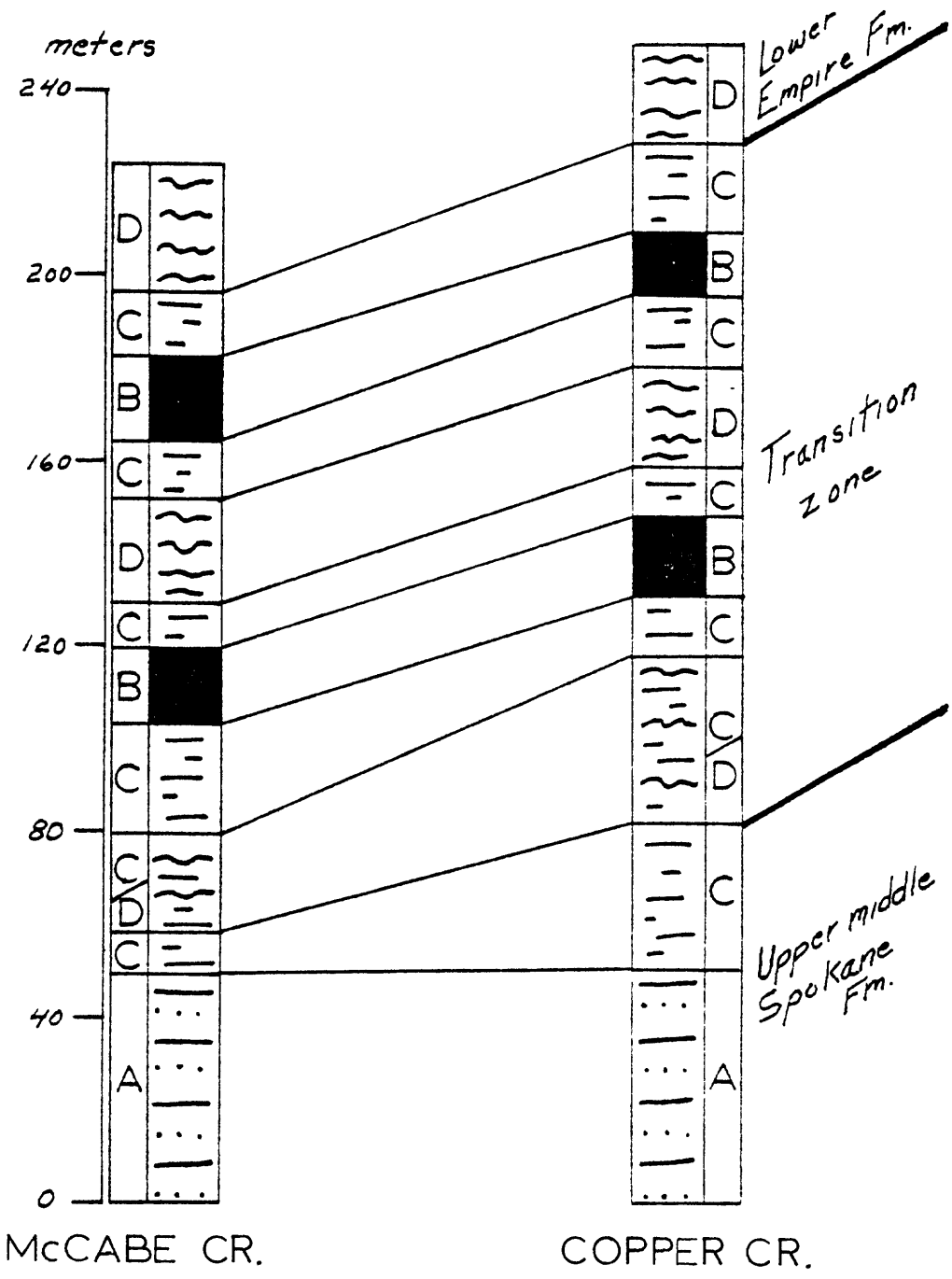

Figure 42.--Correlation of lithofacies between the McCabe and Copper Creek sections, a distance of 25 km; vertical scale, 1 in. = 40 meters.

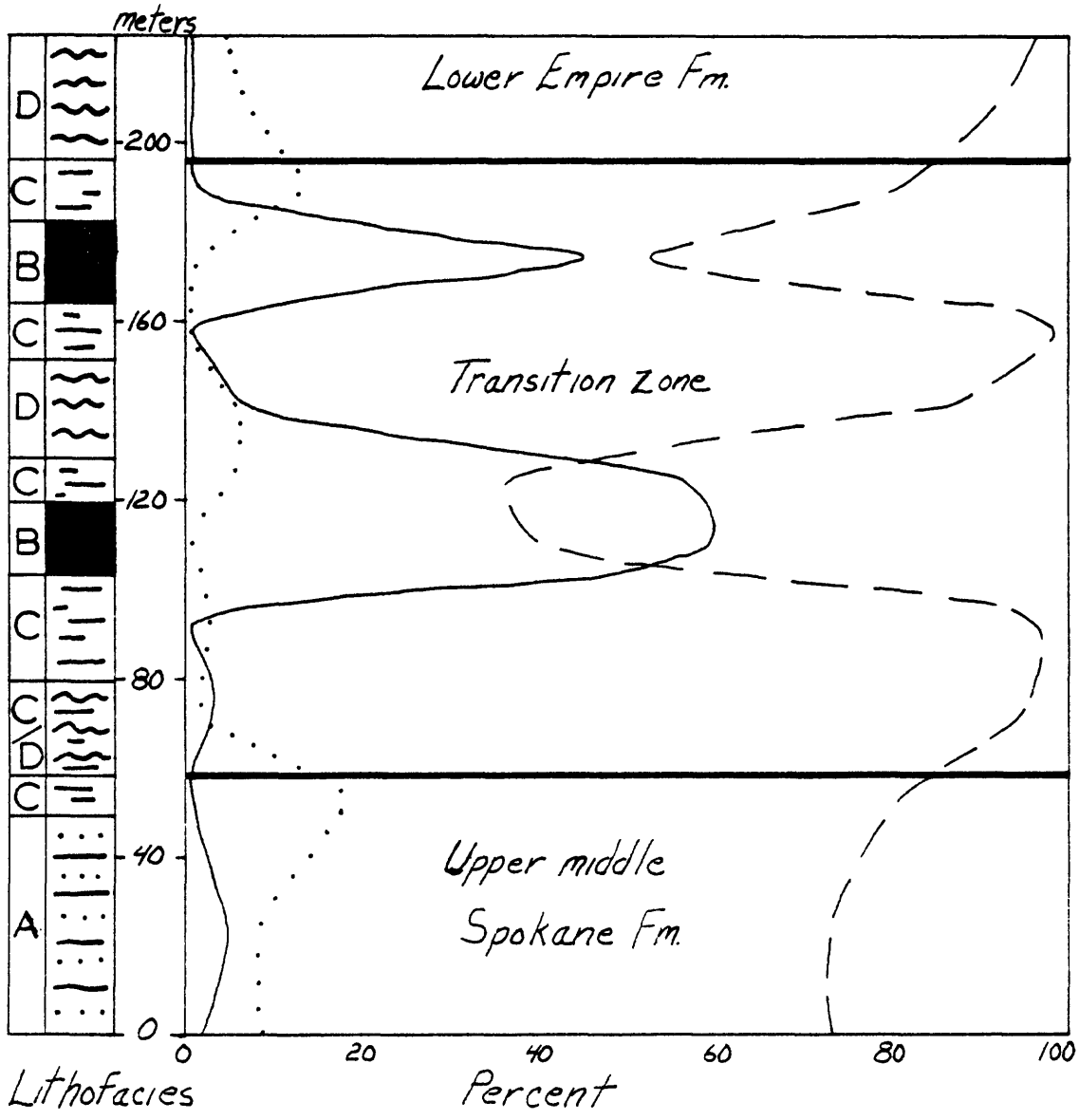

Figure 43.--Distribution and percentage of rock types in the McCabe Creek section. Dots, arenite; dashes, siltite; and solid line, argillite.

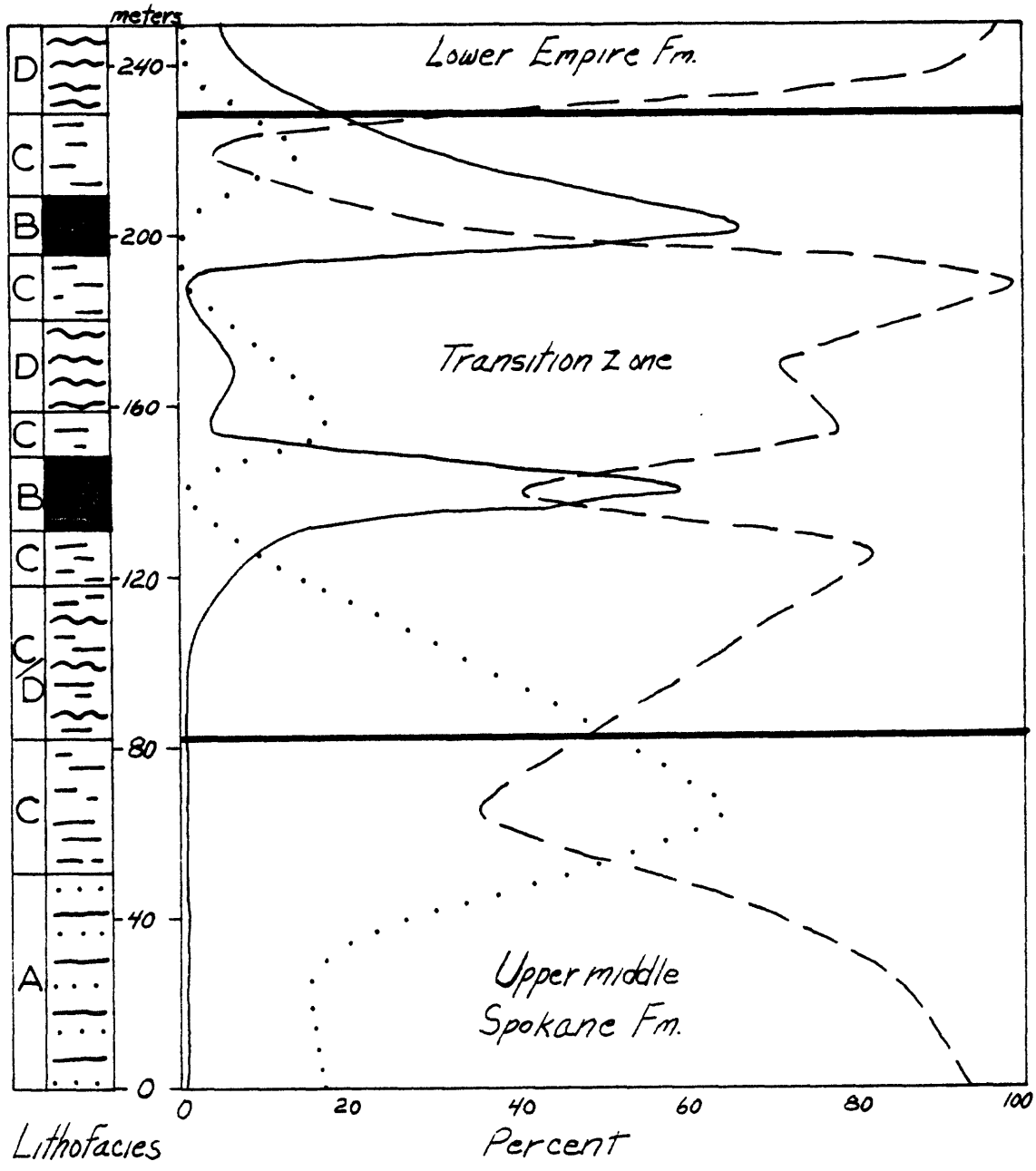

Figure 44.--Distribution and percentage of rock types in the Copper Creek section. Dots, arenite; dashes, siltite; and solid line, argillite.

Several other exposures of the Ys/Ye transition zone were visited across the Belt basin and are shown on figure 1. At Dutcharm Lake, 85 km northwest of McCabe Creek in the Mission Mountains, outcrops expose the upper part of the TZ, particularly lithofacies C. The top of the Spokane Formation, as determined by color, is also marked by sand units very similar to McCabe and Copper Creeks. Sands are medium grained, coarser than other sections, and composed of subrounded quartz in a grain-supported fabric.

At Blacktail Mountain, approximately 50 km northwest of Dutcharm Lake, 22 closely spaced, shallow drill holes penetrated the Ys/Ye transition. Alternating purple and gray sequences with greenish-gray units characterize approximately the upper 40 m of the transition zone. Discontinuous disrupted laminae consisting of graded couplets, generally siltite and argillite, are typical of purplish beds. Greenish units exhibit the normal wavy parallel lamination as graded, fining-upward couplets of siltite and argillite with truncated upper bounding surfaces. Notably absent are sand and mud couplets and sand as thicker arenite units. Fluidization channels are common in the red beds and most consistently at the base and top of green units.

DEPOSITIONAL ENVIRONMENT

Most workers in the Belt basin agree that the Spokane Formation and Empire Formation represent a shallow-water environment (Price, 1964; Boyce, 1973; Winston, 1977; Harrison and Reynolds, 1979). Based on primary sedimentary structures and grain size, environments of deposition depicted for these sediments range from fan deltas to tidal flats having gentle, nearly horizontal slopes. Only Winston (1977) and Harrison and Reynolds (1979) have attempted to relate color to depositional environment. Interpretation of lithofacies in this study permits the use of several criteria necessary for recognition of the environment of deposition.

Lithofacies Interpretation

Lithofacies A

Characteristic fining-upward rhythmic successions of oxidized red sediments are interpreted as fluvial or sheet-wash deposits. Braided, shallow, low-gradient streams deposited these sediments on a featureless delta plain. At McCabe Creek, finer grain size, occasional lenticular lamination, and thinner rhythmic successions suggest a more distal facies than at Copper Creek where successions are thicker, coarser grained at the base, and contain more mudchip breccias and ball-and-pillow structures, indicating stronger current velocities and rapid sedimentation.

Lithofacies B

Thinly laminated argillites in thick succession are representative of upper intertidal environments where mud aggregates from suspension during slack-water periods. The abundance of subaerial shrinkage cracks and mudchip breccia indicates recurrent emergence during tidal cycles. Thin interbedded, irregular arenite units are interpreted as low incipient beach berms formed during storms or more intense tides and wave action.

Lithofacies C

Flaser and lenticular bedding or lamination dominates this red facies and is most diagnostic of intertidal settings. Argillite flasers often contain subaerial shrinkage cracks, suggesting periods of emergence typical of tidal flats. Thicker arenite units of this facies, such as those at the top of the transition zone, represent reworked bottom sediments and are interpreted as lower intertidal to subtidal lag sands formed by waves and possibly longshore currents during marine transgression.

Primary sedimentary structures abound in this facies. Load casts and contorted, diapiric, and ball-and-pillow structures are common indicators of rapid sedimentation and suggest pulses of fluvial deposition onto upper intertidal mud flats. In addition, fluid-escape structures characterize some sequences of this facies and probably were produced near the distal margins of the delta plain.

Thin green siltite and argillite beds are interpreted as tidal pool sediments. Large, shallow tidal pools preserved enough organic matter to produce local reducing conditions and green coloration in sediments. These atypical, green-colored units display even, parallel graded lamination unlike lithofacies D.

Lithofacies D

Thicker green sequences, characterized by wavy, parallel lamination and the absence of subaerial sedimentary structures, are interpreted as subtidal deposits. Green coloration is the result of ferrous chlorites produced in the sediments where the decay of preserved organic matter was instrumental in producing early reducing conditions. The presence of stratabound sulfides demonstrates a reducing environment.

At Copper Creek, algal lamination, birdseye structures, gas expulsion pits, subaqueous shrinkage cracks, and oncolites are unique to green beds and suggest a subtidal environment of deposition.

The base of lithofacies D is typically marked by a thin lag sand formed during marine transgression. A sharp color contrast exists between the lithofacies and underlying red beds, whereas the color boundary at the top exhibits a broad transition into red beds. It is suggested that the top of this lithofacies denotes marine regression and emergence, whereupon ferrous iron in the upper green laminae was partially oxidized producing a transitional boundary.

Wide correlation of this lithofacies (fig. 42) supports the interpretation of a subtidal environment over a broad, uniform shallow shelf. Water depths probably did not exceed 12 m.

Depositional Model

Klein (1971, 1972) has proposed a sedimentary model for peritidal environments where recognition is dependent on prograding tidal deposits showing a fining-upward sequence beginning with crossbedded sands and ending with muds. The depositional model presented in this paper does not fit the model precisely. Some of the major differences, such as the absence of tidal channels, low sand supply, low wave-energy, and tidal currents, preclude the formation of a fining-upward stratification sequence.

Tidal-flat sediments in the Gulf of California are very similar to Ys/Ye transition zone sediments. One exception is the dominance of flaser and lenticular lamination on intertidal flats as opposed to uniform horizontal lamination and bedding that characterizes the Gulf sediments (Thompson, 1975, p. 64). Another exception is the apparent absence of evaporite minerals, especially gypsum. This could be a reflection of aridity, seawater composition, or early diagenetic history. Salt casts are well preserved in younger Belt rocks, but not well documented in the Spokane or Empire Formations.

Interpretation of the lithofacies suggests an arid to semiarid pertidal model as the depositional environment of the Ys/Ye transition zone. Alternation and interspersal of lithofacies C and D within the transition zone indicate cycles of marine transgression and regression across a broad, featureless tidal flat with an ultimate major transgression occurring at the beginning of Empire time.

Figure 45 illustrates the depositional model and environment. The mere magnitude and extent of the environment prevents finding a suitable modern analog, with the partial exception of the Gulf of California after which much of the lithofacies interpretation was made.

Critical to the interpretation of the lithofacies and construction of the depositional model is the nature of red and green coloration in the sediments. Although sediment color at the time of deposition was probably pale brown to brownish gray, such as that seen the Gulf of California (Thompson, 1968), rapid oxidation of exposed and intermittently exposed sediment fixed the iron in the ferric state, oxidized organic matter, and began the reddening process, especially in the absence of much interstitial organic matter competing for oxygen. The formation of ferric oxides and ferric hydroxides from the alteration of ferromagnesian minerals ultimately resulted in red coloration by hematite (Walker and others, 1967).

Arid climates are strong oxidizing environments and promote red bed formation, both continental and nearshore marine (Walker, 1967). Thompson (1975, p. 61) expertly describes this process in the Gulf and in addition comments on the reducing conditions in subtidal environments producing gray sediments. Reduced iron is ultimately bound up in ferrous chlorites, the significant mineral forming green coloration (Harrison and Grimes, 1970). Reducing conditions are most likely produced by the decay of entrapped and preserved organic matter. Final fixing of the bright-red and green hues occurs diagenetically but only as a function of time.

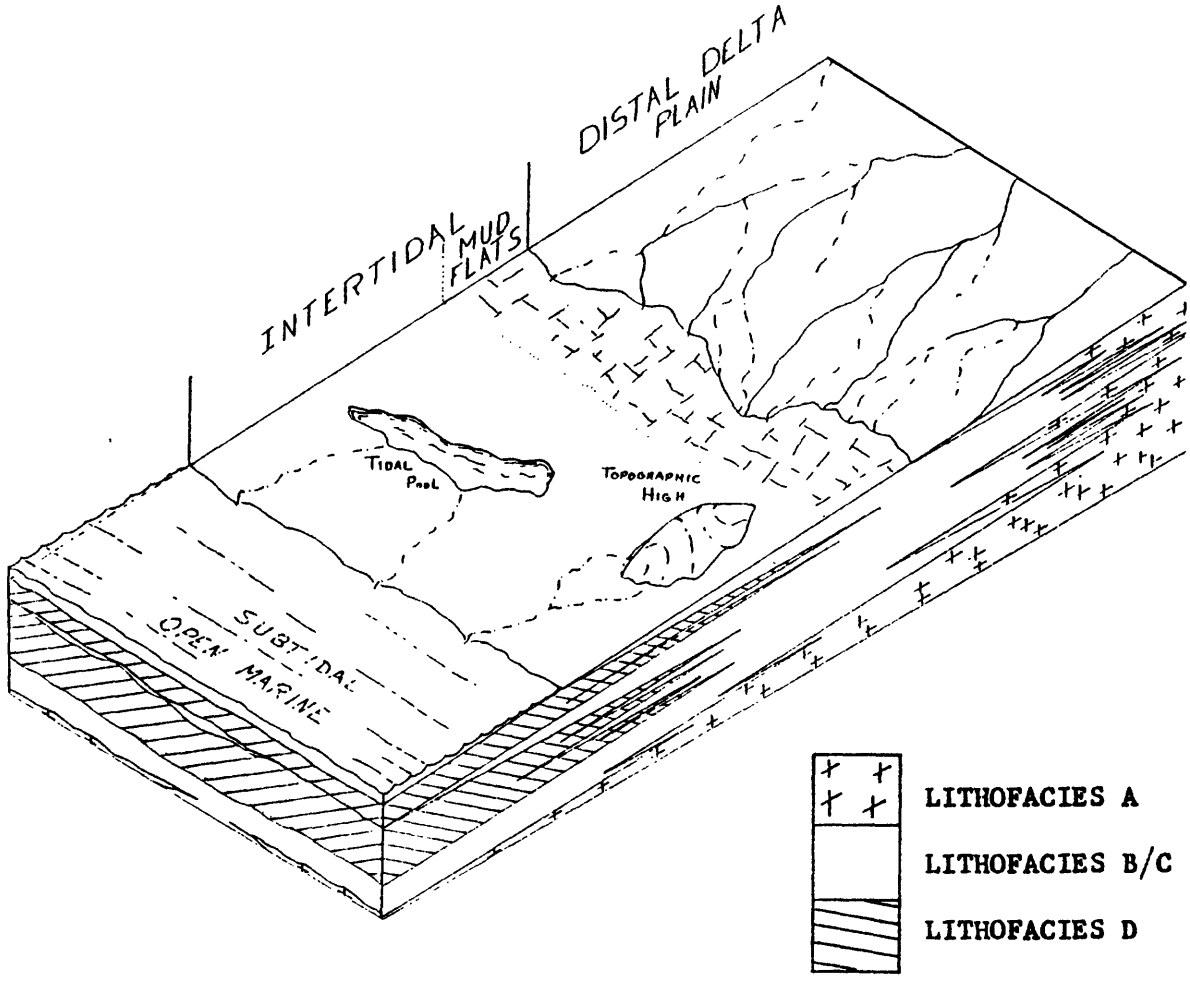

Figure 45.--Peritidal depositional model for the Spokane Formation-Empire Formation transition zone. Model illustrates cyclic marine transgression and regression recorded by the pertidal lithofacies. Horizontal scale in tens of kilometers, vertical scale in tens of meters.

Within the sequences studied, the distribution of primary sedimentary structures confirms this notion. Subaerial structures are found in red beds, subaqueous in green beds. Recent investigations of Belt rocks by Harrison and Reynolds (1979) and work reported by Winston (1977) reach similar conclusions regarding the relations between color of the sediments and their depositional environment.

Of particular consequence is the definition of the Spokane Formation and Empire Formation boundary. Having in the past been defined as a color boundary, one close look at the depositional environment confirms the suspicion that boundaries are diachronous. Willis (1902, p. 332) recognized this problem early while studing the analogous lower Spokane Formation and Greyson Formation boundary and stated, ". . .the line of distinction between them is one diagonal to the stratification."

Apparent unconformities between the Spokane Formation and Helena Formation, as noted earlier, are best understood in light of the depositional model. Distinct topographic highs on the tidal flat acted as islands of oxidized sediments during marine advances (fig. 45). Consequently, green beds of the transition zone and the Empire Formation never were deposited over the highs but lapped onto them. Such an environment might explain the intertonguing relationship observed in the southern Elkhorn Mountains. Only during the major marine advance of Helena time did the red bed highs become inundated. As expected, Helena carbonates would then rest on Spokane red beds. In addition, shoals that developed over and around these highs were active sites for stromatolite growth. This condition is well exposed at Evans Peak, as cited in the introduction.

Cyclic transgressions and regressions recorded by the transition zone were probably caused by eustatic changes in sea level or subtle fluctuations in basin subsidence.

Paleotidal Range

Previous studies of paleotidal ranges in Precambrian rocks have been based on the fining-upward model for prograding shorelines proposed by Klein (1971, 1972). Paleotidal range sequences, identified by Klein, used Holocene analogs from temperate climates, mostly in the lee of barrier islands or protected coastal embayments such as the North Sea Coast. Tidal ranges from these areas rarely exceed 4 m, but occasionally reach a maximum of 15 m, such as observed in the Minas Basin, Bay of Fundy, Nova Scotia (Knight and Dalrymple, 1975). In these environments, the base of a prograding clastic tidal sequence is marked by cross-stratified sands with bipolar-bimodal dip orientation and is terminated upward by silty clays (Klein, 1971, p. 2589).

In the Gulf of California, lack of tidal circulation, sand supply, and wave energy hinder the development of a fining-upward tidal sequence (Thompson, 1975, p. 64). From the type and distribution of surface sediment across the peritidal complex of the Gulf and recognition of gray, burrowed and laminated silt and clay as subtidal sediments, a prograding shoreline should produce a paleotidal range sequence beginning with brown mottled sand and mud, terminating with brown laminated silt and clay (see Thompson, 1968, p. 15-54). Such sequences can be observed in several borings, indicating tidal

ranges from 2 to 3 m (see Thompson, 1968, p. 56, fig. 12). This agrees well with recorded present-day diurnal neap tides in the area of 3 m.

Within the Spokane Formation and Empire Formation transition zone, two episodes of marine regression or shoreline progradation are recognized. Paleotidal range can be identified as the thickness of lithofacies C and B when preceded by lithofacies D or green, subtidal siltites (fig. 42). The average paleotidal range recorded in the stratigraphic sections is 33 m.

Paleotidal range determinations by Klein (1972, p. 397; 1975) for late Precambrian environments range from 0.3 to 13.0 m. By comparison, paleotidal range, as determined above for the transition zone, seems too large; however, exaggerated paleotidal ranges as much as 50 m have been proposed for early Precambrian (2,100 to 3,200 m.y.) peritidal sequences from South Africa using the fining-upward model (Von Brunn and Hobday, 1976; Button and Vos, 1977; Von Brunn and Mason, 1977). In addition, at least one middle Proterozoic tidal sequence in the Arctic Archipelago indicates paleotidal ranges as much as 30 m using the same model (Young and Jefferson, 1975, p. 1742).

Several reasons may account for the exaggerated paleotidal ranges. (1) Tectonic subsidence in the basin caused overthickening or stacking of the measured sequence. (2) Earth-moon distance was shorter, causing increased tidal currents and amplitudes. (3) Shelf widths were more extensive than is presently known and greatly influenced tidal range as suggested by Redfield (1958).

It is postulated that enlarged shelf width and embayment by the epicratonic basin during Ys/Ye time were the determinant factors controlling tidal range, as the effects of either basin subsidence or closer earth-moon distance are not reflected in sediment grain size or sedimentary structures, both of which indicate a low-energy regime. Klein (1977, p. 286) adequately summarizes this situation by stating, "The infracratonic settings of Proterozoic sedimentary basins suggests that shelf width may have been an important control on tidal range."

REFERENCES

Blatt, Harvey, Middleton, Gerard., and Murray, Raymond, 1972, Origin of sedimentary rocks: New Jersey, Prentice Hall Inc., 634 p.

Bowden, T. D., 1977, Depositional processes and environments within the Revett Formation, Precambrian Belt Supergroup, northwestern Montana and northern Idaho: University of California Riverside, M.S. thesis, 161 p.

Boyce, R. L., 1973, Depositional systems in the Ravalli Group--A conceptual model for possible modern analogue, in Belt Symposium, 1973: University of Idaho, v. 1, p. 139-158.

Bradley, W. H., 1929, Algae reefs and oolites of the Green River Formation: U.S. Geological Survey Professional Paper 154-G, p. 203-223.

Bucher, W. H., 1919, On ripples and related sedimentary surface their paleogeographic interpretations: American Journal of Science, v. 47, p. 149-210, 241-269.

Burst, J. F., 1965, Subaqueously formed shrinkage cracks in clay: Journal of Sedimentary Petrology, v. 35, p. 348-353.

Button, Andrew, and Vos, R. G., 1977, Subtidal and intertidal clastic and carbonate sedimentation in a macrotidal environment--An example from the lower Proterozoic of South Africa: Sedimentary Geology, v. 18, p. 175-200.

Campbell, C. V., 1967, Lamina, laminaset, bed, and bedset: Sedimentology, v. 8, p. 7-26.

Clark, A. L., 1971, Stratabound copper sulfides in the Precambrian Belt Supergroup, northern Idaho and northwestern Montana: Mining Geology Japan, Special Issue 3, p. 261-267.

Clifton, H. E., 1969, Beach lamination--Nature and origin: Marine Geology, v. 7, p. 553-559.

Clifton, H. E., Hunter, R. E., and Phillips, R. L., 1971, Depositional structures and processes in the non-barred high-energy nearshore: Journal of Sedimentary Petrology, v. 41, p. 651-670.

Collins, J. A., and Smith, Leigh, 1977, Genesis of cupriferous quartz arenite cycles in the Grinnell Formation (Spokane equivalent), middle Proterozoic (Helikian) Belt-Purcell Supergroup, eastern Rocky Mountains, Canada: Canadian Petroleum Geology Bulletin, v. 25, p. 713-735.

Daley, Brian, 1971, Diapiric and other deformational structures in an Oligocene argillaceous limestone: Sedimentary Geology, v. 6, p. 29-51.

Dangeard, Louis, Migniot, Claude, Larsonneur, Claude, and Baudet, Philippe, 1964, Figures et structures observees au cours du tassement des vases sous l'eau: Comptes rendus hebdomadaires des séances de l'Académie des Sciences, Paris, v. 258, p. 5935-5938.

Dean, W. E., and Eggleston, J. R., 1975, Comparative anatomy of marine and freshwater algal reefs, Bermuda and central New York: Geological Society of America Bulletin, v. 86, p. 665-676.

Deelman, J. C., 1972, On mechanisms causing birdseye structures: Neues Jahrbuch für Geologie und Paläontologie Monatshefte, v. 10, p. 582-595.

Donovan, R. N., and Foster, R. J., 1972, Subaqueous shrinkage cracks from the Cathiness Flagstone Series (Middle Devonian) of northeast Scotland: Journal of Sedimentary Petrology, v. 42, p. 309-317.

Dott, R. H., Jr., and Howard, J. K., 1962, Convolute lamination in nongraded sequences: Journal of Geology, v. 70, p. 114-121.

Dunham, R. J., 1970, Keystone vugs in carbonate beach deposits: American Association of Petroleum Geologists Bulletin, v. 54, p. 845.

Dzulynski, Stanislaw, and Sanders, J. E., 1962, Current marks on firm mud bottoms: Connecticut Academy of Arts and Sciences Transactions, v. 42, p. 57-96.

Dzulynski, Stanislaw, and Simpson, Frank, 1966, Experiments on interfacial current markings: Geologica Romana, v. 5, p. 197-214.

Dzulynski, Stanislaw, and Smith, A. J., 1963, Convolute lamination, its origin, preservation, and directional significance: Journal of Sedimentary Petrology, v. 33, p. 616-627.

Eardley, A. J., 1938, Sediments of Great Salt Lake, Utah: American Association of Petroleum Geologists Bulletin, v. 22, p. 1305-1391.

Earhart, R. L., 1975, Andesite sills in the Red Mountain area, Scapegoat Wilderness, Lewis and Clark County, Montana: U.S. Geological Survey Journal of Research, v. 3, p. 415-424.

Earhart, R. L., Grimes, D. J., Leinz, R. W., and Marks, L. Y., 1977, Mineral resources of the proposed additions to the Scapegoat Wilderness, Powell and Lewis and Clark Counties, Montana: U.S. Geological Survey Bulletin 1430, 62 p.

Eby, D. E., 1977, Sedimentation and early diagenesis within eastern portions of the Middle Belt Carbonate (Helena Formation), Belt Supergroup (Precambrian Y), western Montana: State University of New York at Stony Brook, Ph. D. thesis, 504 p.

Evans, M. E., Bingham, D. K., and McMurry, E. W., 1975, New paleomagnetic results from the Upper Belt-Purcell Supergroup of Alberta: Canadian Journal of Earth Science, v. 12, p. 52-61.

Fenton, C. L., and Fenton, M. A., 1937, Belt series of the North: Stratigraphy, sedimentology, paleontology: Geological Society of America Bulletin, v. 48, p. 1873-1970.

Fischer, A. G., 1975, Tidal deposits, Dachstein limestone of the North-Alpine Triassic, in Ginsberg, R. N., ed., Tidal Deposits: New York, Springer-Verlag, p. 235-242.

Friedman, G. M., and Sanders, J. E., 1978, Principles of sedimentology: New York, John Wiley and Sons, 792 p.

Gavelin, Sven, and Russell, R. V., 1967, Primary sedimentary structures from the Precambrian of Southeastern Sweden: Geologiska Foreningens i Stockholm Forhandlingar, v. 89, p. 74-104.

Gebelein, C. D., 1969, Distribution, morphology, and accretion rate of recent subtidal algal stromatolites, Bermuda: Journal of Sedimentary Petrology, v. 39, p. 49-69.

Ginsberg, R. N., 1975, ed., Tidal Deposits, a casebook of recent examples and fossil counterparts: New York, Springer-Verlag, 428 p.

Glaessner, M. F., 1958, Sedimentary flow structures on bedding planes: Journal of Geology, v. 66, p. 1-7.

Goddard, E. N., Chm., 1979, Rock-color chart: Netherlands, Huyskes-Enschede, 8 p.

Ham, W. E., 1952, Algal origin of the "birdseye" limestone in the Mc-Lish Formation: Oklahoma Academy of Sciences, Proceedings 33, p. 200-203.

Harms, J. C., Southard, J. B., Spearing, and Walker, R. G., 1975, Depositional environments as interpreted from primary sedimentary structures and stratification sequences: Society of Economic Paleontologists and Mineralogists Course No. 2, 161 p.

Harrison, J. E., 1972, Precambrian Belt Basin of northwestern United States--Its geometry, sedimentation, and copper occurrences: Geological Society of America Bulletin, v. 83, p. 1215-1240.

Harrison, J. E., 1974, Copper mineralization in miogeosynclinal clastics of the Belt Supergroup, northwestern United States, in Gisements stratiformes et provinces cupriferes: Geological Society of Belgium Special Publication, p. 353-366.

Harrison, J. E., Griggs, A. B., and Wells, J. D., 1974, Tectonic features of the Precambrian Belt Basin and their influence on Post-Belt Structures: U.S. Geological Survey Professional Paper 866, 15 p.

Harrison, J. E., and Grimes, D. J., 1970, Mineralogy and geochemistry of some Belt rocks, Montana and Idaho: U.S. Geological Survey Bulletin 1312-O, 49 p.

Harrison, J. E., and Reynolds, M. W., 1979, Preliminary geology of the Blacktail Mountain drilling site, Flathead County, Montana: U.S. Geological Survey Open-File Report 79-938, 30 p.

Hoffman, Paul, 1974, Shallow and deep water stromatolites in a lower Proterozoic platform-to-basin facies changes, Great Slave Lake, Canada: American Association of Petroleum Geologists Bulletin 58, p. 856-867.

_____1975, Shoaling-upward shale-to-dolomite cycles in the Rocknest Formation (Lower Proterozic), Northwest Territories, Canada, in Ginsberg, R. N., ed., Tidal Deposits: New York, Springer-Verlag, 428 p.

Hrabar, S. V., 1971, Stratigraphy and depositional environment of the St. Regis Formation of the Ravalli Group (Precambrian Belt Megagroup) northwestern Montana and Idaho: University of Cincinnati, Ph. D. thesis, 92 p.

_____1973, Deep-water sedimentation in the Ravalli Group (Late pЄ Belt Megagroup) northwestern Montana, in Belt Symposium, 1973: University of Idaho, v. II, p. 67-81.

Illing, L. V., 1959, Deposition and diagenesis of some Upper Paleozoic carbonate sediments in western Canada: Fifth World Petroleum Congress Proceedings, sec. 1, p. 23-50.

Jopling, A. V., and Walker, R. G., 1968, Morphology and origin of ripple-drift cross-lamination, with examples from the Pleistocene of Massachusetts: Journal of Sedimentary Petrology, v. 38, p. 971-984.

Kindle, E. M., 1916, Small pit and mound structures developed during sedimentation: Geological Magazine, v. 3, p. 542-547.

_____1917, Diagnostic characteristics of marine clastics: Geological Society of America Bulletin, v. 28, p. 905-916.

Klein, G. de V., 1965, Diverse origins of graded bedding: Geological Society of America Special Paper 82, p. 1-112.

_____1970, Tidal origin of a Precambrian quartzite--the lower fine grained quartzite (Dalradian) of Islay, Scotland: Journal of Sedimentary Petrology, v. 40, p. 973-985.

_____1971, A sedimentary model for determining paleotidal range: Geological Society of America Bulletin, v. 82, p. 2585-2592.

_____1972, Determination of paleotidal range in clastic sedimentary rocks: 24th International Geological Congress Proceedings, sec. 6, p. 397-405.

_____1975, Paleotidal Range sequences, middle member, Wood Canyon Fm (late pЄ, eastern California and western Nevada, in Ginsberg, R. N., ed., Tidal Deposits: New York, Springer-Verlag, p. 171-177.

_____1977, Epilogue: Sedimentary Geology, v. 18, p. 283-287.

Klepper, M. R., Weeks, R. A., and Ruppel, E. J., 1957, Geology of the southern Elkhorn Mountains, Jefferson and Broadwater Counties, Montana: U.S. Geological Survey Professional Paper 292, 82 p.

Knight, R. J., and Dalrymple, R. W., 1975, Intertidal sediments from the south shore of Cobequid Bay, Bay of Fundy, Nova Scotia, Canada, in Ginsberg, R. N., ed., Tidal Deposits: New York, Springer-Verlag, p. 47-55.

Kuenen, P. H., 1957, Sole markings of graded graywacke beds: Journal of Geology, v. 65, p. 231-258.

_____1965, Value of experiments in geology: Geologie en mijnbouw, v. 44, p. 22-36.

_____1966, Experimental turbidite lamination in a circular flume: Journal of Geology, v. 74, p. 523-545.

Laporte, L. F., 1967, Carbonate deposition near mean sea-level and resultant facies mosaic: Manlius Formation (lower Devonian) of New York State: American Association of Petroleum Geologists Bulletin 51, p. 73-101.

Logan, B. W., 1961, Cryptozoan and associated stromatolites from the recent, Shark Bay, western Australia: Journal of Geology, v. 69, p. 517-533.

Logan, B. W., Hoffman, Paul, and Gebelein, C. D., 1974, Algal mats, cryptalgal fabrics and structures, Hamelin Pool, western Australia: American Association of Petroleum Geologists Memoir 22, p. 140-194.

Logan, B. W., Rezak, Richard, and Ginsberg, R. N., 1964, Classification and environmental significance of algal stromatolites: Journal of Geology, v. 72, p. 68-83.

Lowe, D. R., 1975, Water escape structures in coarse-grained sediments: Sedimentology, v. 22, p. 157-204.

McGowen, J. H., 1970, Gum Hollow Fan Delta, Nueces Bay, Texas: Bureau of Economic Geology, University of Texas, Report of Investigations No. 69, 91 p.

McKee, E. D., 1965, Experiments on ripple lamination, in Middleton, G. V., ed., Primary sedimentary structures and their hydrodynamic interpretation: Society of Economic Paleontologists and Mineralogists, Special Publication 12, p. 66-83.

McKee, E. D., and Goldberg, M., 1969, Experiments on formation of contorted structures in mud: Geological Society of America Bulletin, v. 80, p. 231-244.

Maxwell, D. T., and Hower, John, 1967, High-grade diagenesis and low-grade metamorphism of illite in the Precambrian Belt Series: American Mineralogist, v. 52, p. 843-857.

Mertie, J. B., Jr., Fischer, R. P., and Hobbs, S. W., 1951, Geology of the Canyon Ferry quadrangle, Montana: U.S. Geological Survey Bulletin 972, 99 p.

Mudge, M. R., 1970, Origin of the Disturbed Belt in northwestern Montana: Geological Society of America Bulletin, v. 81, p. 377-392.

Mudge, M. R., and Earhart, R. L., in press, The Lewis thrust fault and related structures in the Lewis and Clark Range, northwestern Montana: U.S. Geological Survey Professional Paper.

Mudge, M. R., Earhart, R. L., Watts, K. C., Jr., Tuchek, E. T., and Rice, W. L., 1974, Mineral resources of the Scapegoat Wilderness, Powell and Lewis and Clark Counties, Montana: U.S. Geological Survey Bulletin 1385-B, 82 p.

Mudge, M. R., Earhart, R. L., Whipple, J. W., and Harrison, J. E., in press, Geologic map of the Choteau 1^{o} x 2^{o} quadrangle, Lewis and Clark, Teton, Powell, Missoula, Lake, Flathead, and Cascade Counties, Montana: U.S. Geological Survey Map I- .

Mudge, M. R., Erickson, R. L., and Kleinkopf, D., 1968, Reconnaissance geology, geophysics, and geochemistry of the southern part of the Lewis and Clark range, Montana: U.S. Geological Survey Bulletin 1252-E, 35 p.

Obradovich, J. D., and Peterman, Z. E., 1968, Geochronology of the Belt Series, Montana: Canadian Journal of Earth Sciences, v. 5, p. 737-747.

Pettijohn, F. J., and Potter, P. E., 1964, Atlas and glossary of primary sedimentary structures: New York, Springer-Verlag, 370 p.

Pettijohn, F. J., Potter, P. E., and Siever, Raymond, 1973, Sand and sandstone: New York, Springer-Verlag, 618 p.

Picard, M. D., 1966, Oriented, linear-shrinkage cracks in Green River Formation (Eocene), Raven Ridge area, Uinta Basin, Utah: Journal of Sedimentary Petrology, v. 36, p. 1050-1057.

Picard, M. D., and High, L. R., 1969, Some sedimentary structures resulting from flash floods: Guidebook of Northern Utah, Bulletin 82, p. 175-190.

Playford, P. E., and Cockbain, A. E., 1969, Deepwater forms in the Devonian of Western Australia: Science 165, p. 1008-1010.

Potter, P. E., and Pettijohn, F. J., 1977, Paleocurrents and basin analysis: New York, Springer-Verlag, 425 p.

Price, R. A., 1964, The Precambrian Purcell System in the Rocky Mountains of southern Alberta and British Columbia: Bulletin of Canadian Petroleum Geology, v. 12, p. 399-426.

Redfield, A. C., 1958, The influence of the continental shelf on the tides of the Atlantic Coast of the United States: Journal of Marine Research, v. 17, p. 432-448.

Reineck, H.-E., 1967, Layered sediments of tidal flats, beaches, and shelf bottoms of the North Sea, in Lauff, George H., ed., Estuaries: American Association for the Advancement of Science, Publication No. 83, p. 191-206.

Reineck, H.-E., 1969, Die entstehung von Runzelmarken: Natur und Museum, v. 99, p. 386-388.

_____1975, German North Sea tidal flats, in Ginsberg, R. N., ed., Tidal Deposits: New York, Springer-Verlag, p. 5-12.

Reineck, H.-E., and Singh, I. B., 1972, Genesis of laminated sand and graded rhythmites in storm-sand layers of shelf mud: Sedimentology, v. 18, p. 123-128.

_____1975, Depositional sedimentary environments: New York, Springer-Verlag, 439 p.

Reineck, H.-E., and Wunderlich, Friedrich, 1968, Classification and origin of flaser and lenticular bedding: Sedimentology, v. 11, p. 99-104.

Ross, C. P., 1959, Geology of Glacier National Park and the Flathead region, northwestern Montana: U.S. Geological Survey Professional Paper 296, 125 p.

_____1963, The Belt Series in Montana: U.S. Geological Survey Professional Paper 346, 122 p.

Shinn, E. A., 1968, Practical significance of birdseye structures in carbonate rocks: Journal of Sedimentary Petrology, v. 38, p. 215-223.

Shrock, R. R., 1948, Sequence in layered rocks: New York, McGraw-Hill, 507 p.

Singh, I. B., 1969, Primary sedimentary structures in pЄ quartzites of Telemark, southern Norway, and their environmental significance: Norsk Geologisk Tidsskrift, v. 49, p. 1-31.

Sorauf, J. E., 1965, Flow rolls of upper Devonian rocks of south-central New York state: Journal of Sedimentary Petrology, v. 35, p. 553-563.

Swarbrick, E. E., 1968, Physical diagenesis; intrusive sediment and connate water: Sedimentary Geology, v. 2, p. 161-175.

Tanner, W. F., 1960, Shallow water ripple mark varieties: Journal of Sedimentary Petrology, v. 30, p. 481-485.

Terwindt, J. H. J., and Breusers, H. N. C., 1972, Experiments on the origin of flaser, lenticular, and sand-clay alternating bedding: Sedimentology, v. 19, p. 85-98.

Thompson, R. W., 1968, Tidal flat sedimentation on the Colorado River Delta, northwest Gulf of California: Geological Society of America Memoir 107, 133 p.

_____1975, Tidal flat sediments of the Colorado River Delta, northwestern Gulf of California, in Ginsberg, R. N., ed., Tidal Deposits: New York, Springer-Verlag, p. 57-65.

Trammell, J. W., 1975, Strata-bound copper mineralization in the Empire Formation and Ravalli Group, Belt Supergroup, northwest Montana: University of Washington, Ph. D. thesis, 70 p.

Van Straaten, L. M. J. U., 1954, Composition and structure of Recent marine sediments in the Netherlands: Leidse Geologische Medelingen, v. 19, p. 1-110.

Vitorello, Icaro, and Van der Voo, Rob, 1977, Late Hadrynian and Helikian pole positions from the Spokane Formation, Montana: Canadian Journal of Earth Sciences, v. 14, p. 67-73.

Von Brunn, Victor, and Hobday, D. K., 1976, Early Precambrian tidal sedimentation in the Pongola Supergroup of South Africa: Journal of Sedimentary Petrology, v. 46, p. 670-679.

Von Brunn, Victor, and Mason, T. R., 1977, Siliciclastic-carbonate tidal deposits from the 3,000 m.y. Pongola Supergroup, South Africa: Sedimentary Geology, v. 18, p. 245-255.

Walcott, C. D., 1899, Precambrian fossiliferous formations: Geological Society of America Bulletin, v. 10, p. 199-244.

Walker, T. R., 1967, Formation of red beds in modern and ancient deserts: Geological Society of America Bulletin 78, p. 353-368.

Walker, T. R., Ribbe, P. H., and Honea, R. M., 1967, Geochemistry of hornblende alteration in Pliocene red beds, Baja California, Mexico: Geological Society of America Bulletin, v. 78, p. 1055-1060.

White, W. A., 1961, Colloid phenomena in sedimentation of argillaceous rocks: Journal of Sedimentary Petrology, v. 31, p. 560-570.

Willis, Bailey, 1902, Stratigraphy and structure, Lewis and Livingston Ranges: Geological Society of America Bulletin, v. 13, p. 305-352.

Winston, D., 1977, Alluvial fan, shallow water, and sub-wave base deposits of the Belt Supergroup near Missoula, Montana: Geological Society of America, Rocky Mountain Section, 30th Annual Meeting, May 14 and 15, 1977, Field Guide No. 5, 41 p.

Young, G. M., and Jefferson, C. W., 1975, Late Precambrian shallow water deposits, Banks and Victoria Islands, Arctic Archipelago: Canadian Journal of Earth Sciences, v. 12, p. 1734-1748.

APPENDICES

Appendix A, Terminology

Terminology used in describing the lithologic properties of measured sections was adopted from the following sources:

Rock name, modified after Pettijohn and others (1973, p. 158) and Harrison and Grimes (1970, p. 3).
Color, rock color chart; Geol. Soc. America, 1970.
Carbonate content, subject field observation with 10 percent HCl.
Grain size, Wentworth size class in millimeters.
Grain rounding and sorting, Pettijohn and others (1973, p. 585-586).
Bedding and lamination, Reineck and Singh (1975, p. 83) and Campbell (1967, p. 18).

Appendix B, Stratigraphic Sections

McCabe Creek Section

The McCabe Creek section is located approximately 15.3 km north of Ovando, Montana. Access is gained by 12.9 km of dirt road and 2.4 km of U.S. Forest Service trail. Exposure is on a south facing spur ridge between McCabe Creek and a small tributary (fig. 46). The transition zone has approximately 97 percent outcrop exposure, most of which has moderate lichen cover.

Figure 47 depicts the geologic setting of the section. A gabbroic sill is approximately 540 m (topographic measure) below the starting point of the section and has had negligible effect on the sediments of the transition zone.

The total exposure measured amounts to 223.87 m. The transition zone begins 57.94 m up from the bottom of the measured section and ends 27.35 m below the top, comprising a thickness of 138.58 m. Empire strata constitute the upper 27.35 m of the section.

Figure 46.--A view of the McCabe Creek exposures used for measurement and description.

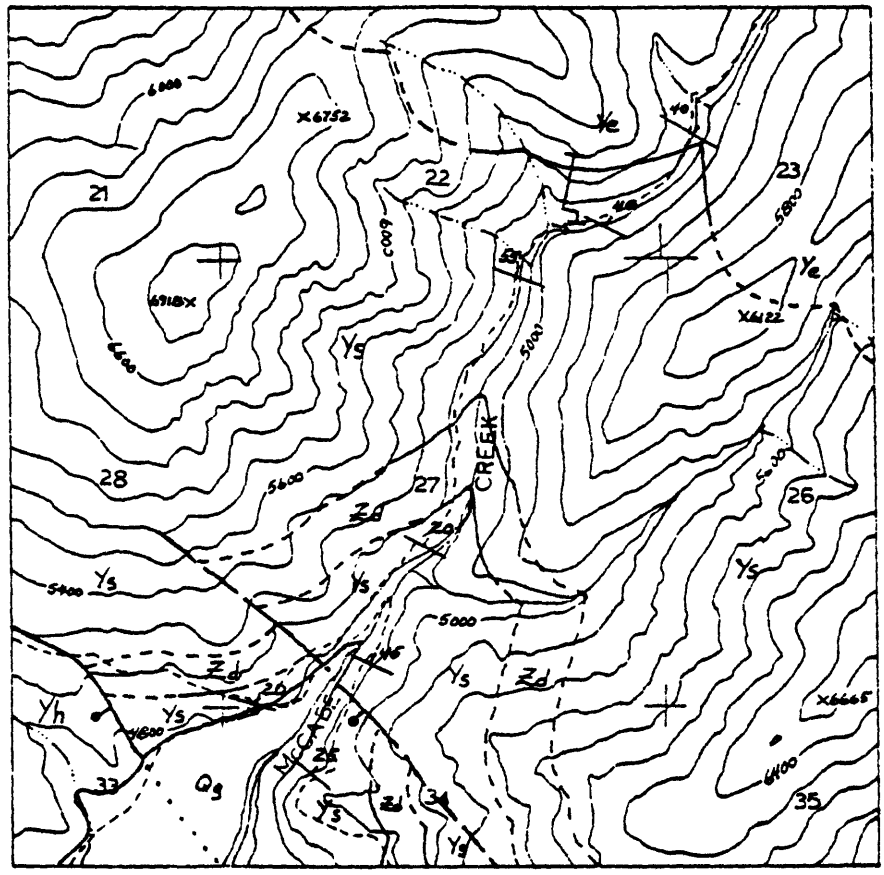

Qg Glacial material (Quaternary)

Zd Diorite sill (Proterozoic Z)

Yh Helena Formation
Ye Empire Formation — (Proterozoic Y)
Ys Spokane Formation

Contact Dashed where approximate

Fault Bar and ball on downthrown side; dotted where concealed, dashed where approximate

40 Strike and dip

Line of measured section

0 .5 1
Kilometers

Figure 47.--Geologic map of the McCabe Creek area and location of measured section.

Empire Formation, lower part (Middle Proterozoic):	Thickness (equivalents) Meters	Feet
15. Siltite, greenish-gray (5G 6/1); slightly calcareous; medium grained; very thick (75 mm) to medium lamination	3.8	12.46
14. Quartz arenite, greenish-gray; slightly calcareous; very fine grained; ripple laminated with coarse siltite	.65	2.13
13. Siltite; same as unit 15	3.3	10.82
12. Siltite, greenish-gray; slightly calcareous; thin lamination with minor interlaminated argillite; syneresis cracks in argillites	2.95	9.68
11. Quartz arenite, dark-greenish-gray (5G 4/1); slightly calcareous; very fine grained; interbedded, and interlaminated coarse to fine siltite; some hackly cleavage in fine siltite	1.3	4.26
10. Siltite; same as unit 12	1.45	4.76
9. Siltite, greenish-gray to dark-greenish-gray; slightly calcareous; thin lamination with prominent hackly cleavage	.73	2.39
8. Siltite, greenish-gray; slightly calcareous; medium grained; very thick (85 mm) lamination; interlaminated lenticular stringers of microspar as birdseye structure	1.1	3.61
7. Siltite, greenish-gray; slightly calcareous; ripple and wavy lamination, thin to medium	5.1	16.73
6. Quartz arenite, very light gray (N8); fine grained, well sorted; subrounded grains; ripple crossbedded	.1	.33
5. Siltite, greenish-gray; slightly calcareous; ripple, wavy, and lenticular lamination, thin to medium; some milky quartz veinlets	2.4	7.87

Empire Formation, lower part--Continued	Thickness (equivalents) Meters	Feet
4. Siltite, greenish-gray; slightly calcareous; coarse grained; ripple laminated; stratabound limonite after pyrite in cubic casts (3-4 mm)	.115	.38
3. Siltite; same as unit 7	2.05	6.72
2. Siltite; same as unit 4	.4	1.31
1. Siltite, greenish-gray; slightly calcareous; medium to fine grained; wavy, thin lamination; interlaminated ripple very fine grained arenite	1.9	6.25
Total thickness of the lower part	27.35	89.71

Spokane Formation (Middle Proterozoic) Transition zone (contact with overlying Empire Formation conformable):	Thickness (equivalents) Meters	Feet
63. Subfeldspathic arenite, moderate-light-gray (N7.5); very fine grained; thin bedding	0.455	1.49
62. Siltite, grayish-red (10R 4/2); coarse grained; minor interlaminated very fine grained arenite	.73	2.39
61. Siltite, moderate-grayish-pink (5R 7/2) to tan weathering; slightly calcareous; medium grained; medium lamination	1.7	5.58
60. Siltite, moderate-grayish-pink; slightly calcareous; medium to fine grained; thin to very thin lamination, hackly cleavage	4.08	13.38
59. Siltite, grayish-red; coarse grained; medium lamination	1.25	4.1
58. Subfeldspathic arenite; same as unit 63	.1	.33
57. Siltite, moderate-grayish-pink; slightly calcareous; coarse to fine grained; medium to thin lamination; interlaminated argillite and minor very fine grained arenite; some desiccation cracks	4.1	13.45
56. Subfeldspathic; same as unit 63	1.5	4.92
55. Covered	.75	2.46
54. Siltite, grayish-red; fine to minor coarse grained; intermittently calcareous; thin and ripple lamination; interlaminated argillite; desiccation cracks; hackly cleavage	7.25	23.78
53. Subfeldspathic arenite; same as unit 63	.075	.25
52. Siltite; same as unit 54	.78	2.56
51. Siltite, moderate-grayish-pink to tan weathering; calcareous; coarse grained; thin to medium lamination; minor interlaminated very fine grained arenite; hackly cleavage	.8	2.62

Transition zone--Continued	Thickness (equivalents) Meters	Feet
50. Argillite, grayish-red; slightly calcareous; thin lamination; hackly cleavage	1.7	5.58
49. Subfeldspathic arenite; same as unit 63	.1	.83
48. Argillite, moderate-grayish-pink; slightly calcareous; interlaminated siltite; desiccation cracks	2.45	8.04
47. Subfeldspathic arenite, pale-green (10G 6/2); slightly calcareous; very fine grained	.045	.15
46. Argillite; same as unit 48	3.5	11.48
45. Siltite, grayish-red; slightly calcareous; coarse to medium grained; thin and ripple lamination; interlaminated very fine grained arenite	5.75	18.86
44. Siltite, grayish-red; slightly calcareous; interlaminated argillite in rhythmic succession; successions average 2.5 m	7.4	24.27
43. Subfeldspathic arenite, medium greenish-gray (5G 5/1); slightly calcareous; very fine grained; ripple laminated with coarse siltite	1.08	3.54
42. Argillite; same as unit 48	.48	1.57
41. Siltite, moderate-grayish-green (10G 5/2); slightly calcareous; coarse to medium grained; wavy to lenticular lamination, thin	11.05	36.24
40. Siltite, dark-greenish-gray (5G 4/1); slightly calcareous; fine grained; thin lamination; hackly cleavage	1.4	4.59
39. Siltite, moderate-grayish-green; slightly calcareous; thin to medium lamination; stratabound chalcocite, bornite(?), and malachite	2.2	7.22

Transition zone--Continued	Thickness (equivalents) Meters	Feet
38. Siltite, moderate-grayish-green; slightly calcareous; coarse grained; thin to medium lamination; minor interlaminated very fine grained arenite	1.3	4.26
37. Subfeldspathic arenite; same as unit 63	.3	.98
36. Argillite, dusky-red (5R 3/4); minor interlaminated coarse siltite; mudchip breccia, desiccation cracks	.9	2.95
35. Siltite, moderate-grayish-green (10G 5/2) to medium-greenish-gray (5G 5/1); coarse to medium grained; thin to medium lamination; minor interlaminated argillite, hackly cleavage	4.5	14.76
34. Argillite; same as unit 50	2.1	6.89
33. Argillite, dusky-red; interlaminated grayish-red siltite; desiccation cracks and mudchip breccia common	3.7	12.14
32. Siltite; same as unit 59	1.37	4.49
31. Siltite; banded grayish-green (5G 5/2) and pale-pink (5RP 8/2), 2-10 mm bands; thin to very thin lamination	.68	2.23
30. Siltite; same as unit 33	1.65	5.41
29. Subfeldspathic arenite, medium-brownish-gray (5YR 5/1); very fine grained; thin bedding; load structures at base	.6	1.97
28. Argillite; same as unit 33	15.85	51.99
27. Siltite; same as unit 59	2.2	7.22
26. Subfeldspathic arenite, medium-brownish-gray; fine to very fine grained, well sorted; subangular to subrounded grains; interbedded and interlaminated coarse siltite; some milky quartz veinlets	.8	2.62
25. Siltite, grayish-red-purple (5RP 4/2); slightly calcareous; interlaminated argillite; thin lamination; desiccation cracks and water-escape channels	1.2	3.94

Transition zone--Continued		Thickness (equivalents)	
		Meters	Feet
24.	Siltite; same as unit 59	1.05	3.44
23.	Siltite, grayish-red-purple to medium-brownish-gray; slightly calcareous; coarse to fine grained; ripple and lenticular lamination with fine to very fine grained arenite and argillite; some flaser bedding	5.8	19.02
22.	Siltite; same as unit 59	5.0	16.4
21.	Siltite, grayish-red to grayish-red-purple; slightly calcareous; coarse to fine grained; interlaminated argillite as graded rhythmites; rhythmic succession ranges from 100 mm to 140 mm	1.65	5.41
20.	Siltite, medium-brownish-gray to grayish-red-purple; intermittently calcareous; coarse grained; interbedded and interlaminated very fine grained arenite; minor argillite; minor ripple cross lamination	4.8	15.74
19.	Siltite, grayish-red-purple; fine grained; thin lamination; hackly cleavage	1.65	5.41
18.	Siltite, pale-blue-green (5BG 7/2); calcareous; fine grained; thin to medium lamination	.72	2.36
17.	Siltite, grayish-red-purple; coarse grained; interbedded very fine grained arenite	1.2	3.94
16.	Siltite, grayish-red; medium to fine grained; thin lamination	3.1	10.17
15.	Siltite; same as unit 18	.25	.82
14.	Siltite; same as unit 16	.3	.98
13.	Siltite; same as unit 18	.5	1.64
12.	Siltite, grayish-red; coarse grained; medium lamination; minor interlaminated argillite	2.9	9.51

Transition zone--Continued	Thickness (equivalents) Meters	Feet
11. Siltite; same as unit 18	0.46	1.51
10. Siltite, grayish-red-purple; coarse to fine grained; interlaminated and ripple laminated very fine grained arenite and argillite as graded rhythmites; rhythmic succession averages 1 m	1.9	6.23
9. Siltite; same as unit 18	.555	1.82
8. Siltite; same as unit 12	1.2	3.94
7. Siltite, pale-blue-green; slightly calcareous in part; coarse to fine grained; thin to very thick lamination; hackly cleavage; very fine grained arenite at top; stratabound copper sulfides	1.695	5.56
6. Siltite, grayish-red-purple; coarse grained; ripple lamination; interlaminated fine to very fine grained arenite with minor argillite; some load structures	1.63	5.35
5. Siltite, pale-blue-green; upper part slightly calcareous; coarse to medium grained; some ripple lamination; interbedded fine to very fine grained, well sorted, and subrounded quartz arenite at base (5YR 7/1); stratabound copper sulfides	2.27	7.45
4. Argillite, dusky-red-purple (5RP 3/2); calcareous; very thin lamination (0.5 mm)	.65	2.13
3. Subfeldspathic arenite, medium-light-gray (N6) to grayish-red-purple (5RP 4/2); calcareous to slightly calcareous; thick lamination	.43	1.41
2. Siltite, grayish-red-purple; calcareous to slightly calcareous; thin lamination; interlaminated argillite	.8	2.62
1. Siltite, pale-green (10G 7/2); slightly calcareous; medium lamination	.2	.63
Total thickness of Transition zone	138.58	454.54

Spokane Formation, upper middle part (Middle Proterozoic):	Thickness (equivalents) Meters	Feet
24. Subfeldspathic arenite, medium-light-gray (N6) to grayish-red-purple (5RP 4/2); calcareous to slightly calcareous; thick lamination	0.8	2.62
23. Siltite, grayish-red-purple; calcareous to slightly calcareous; thin to medium ripple lamination; interlaminated argillite; some flaser bedding	3.7	12.14
22. Quartz arenite, medium-light-gray; calcareous to slightly calcareous; fine to very fine grained; subrounded to rounded; minor interlaminated siltite	.87	2.85
21. Siltite, grayish-red-purple; medium grained; ripple laminated, lenticular, well sorted, fine to very fine grained arenite; interlaminated argillite with desiccation cracks and mudchip breccia; well developed ball-and-pillow structures and flame structure	3.645	11.96
20. Covered	2.74	8.99
19. Subfeldspathic arenite, light-gray (N7) to very-light-gray (N8); slightly calcareous; very fine grained; minor tangential crossbedding	.5	1.64
18. Siltite, grayish-red-purple; coarse grained; interbedded very fine grained arenite	.9	2.95
17. Subfeldspathic arenite, medium-light-gray (N6); very fine grained; thin bedding; interbedded coarse siltite as graded rhythmites	.95	3.12
16. Siltite; same as unit 18	.75	2.46
15. Siltite, grayish-red-purple; ripple and lenticular lamination with interlaminated very fine grained arenite and argillite; desiccation cracks and mudchip breccia in argillite	3.95	12.96

Spokane Formation, upper middle part--Continued	Thickness (equivalents) Meters	Feet
14. Subfeldspathic arenite, grayish-red-purple (5RP 4/2); very fine grained; grading upwards in rhythmic succession to siltite and argillite. Nested couplets of arenite/siltite and siltite/argillite, average 20 mm	2.3	7.54
13. Argillite, grayish-red-purple; minor interlaminated siltite; minor desiccation cracks and mudchip breccia	2.4	7.87
12. Quartz arenite, grayish-blue-green 5BG 6/2) to grayish-orange-pink (YR 8/1); fine grained, well sorted; subrounded to rounded grains	.06	.2
11. Siltite; same as unit 15	13.55	44.44
10. Covered	3.53	11.58
9. Siltite, pale-red-purple (5RP 6/2) to grayish-red (5R 4/2); thin to medium lamination; interlaminated argillite	2.7	8.86
8. Subfeldspathic arenite, pale-purple (5P 6/2); very fine grained; thin to medium bedding; ripple cross lamination in top 10 cm	.3	.98
7. Siltite, grayish-red-purple; coarse to minor fine grained; minor interbedded and interlaminated argillite to graded rhythmites; some desiccation cracks, mudchip breccia, and water-escape channels in argillite	4.35	14.27
6. Siltite, grayish-red-purple; fine grained; thin lamination; hackly cleavage	.87	2.85
5. Siltite; same as unit 7	1.07	3.51
4. Siltite; same as unit 6	1.18	3.87
3. Siltite; same as unit 7	4.15	13.61

Spokane Formation, upper middle part--Continued	Thickness (equivalents) Meters	Feet
2. Subfeldspathic arenite, medium-light-gray (N6) to pale-purple (5P 6.5/2); very fine grained; lenticular	.075	.25
1. Siltite; same as unit 7	2.6	8.53
Partial thickness of upper middle Spokane Formation	57.94	190.04

Copper Creek Section

The Copper Creek section is exposed along a northeast-trending ridge dividing the headwaters of Copper Creek and Meadow Creek. From Lincoln, Montana, access is provided by 33 km of mostly dirt road up the Copper Creek drainage. A jeep trail continues 4 km on to Copper Camp where a short 1.5 km hike along the ridge brings you to the measured exposures (fig. 48).

Outcrops along the south-facing slope of the ridge have the best exposure where the transition zone is 93 percent exposed with light lichen cover. Early in the summer, some of the exposure is covered with snow drifts, especially near the ridge line.

The measured section is faulted several times by small displacement normal faults trending northwest and having the west side down. These faults conveniently provide better exposure by repeating portions of the section along the ridge. Bedding strikes obliquely to the ridge line and dips gently eastward 13 degrees to 25 degrees (fig. 49).

One small (3.73 m thick) meta-andesite sill intrudes the section. These sills are common in this area and are considered to be Proterozoic Y age (Earhart, 1975). Metamorphic effects extend less than 1 m into the enclosing rocks creating a bleached calc-hornfels.

As in the other measured section, measurement begins below the lowest visible green bed sequence and extends upward into the Empire Formation. The total thickness measured is 250.61 m of which the Empire Formation constitutes 20.74 m, the transition zone 144.15 m, meta-andesite sill 3.73 m, and upper middle Spokane Formation 81.96 m.

Figure 48.--Copper Creek exposures looking north. Offsets neccessary for measuring the total section were made eastward.

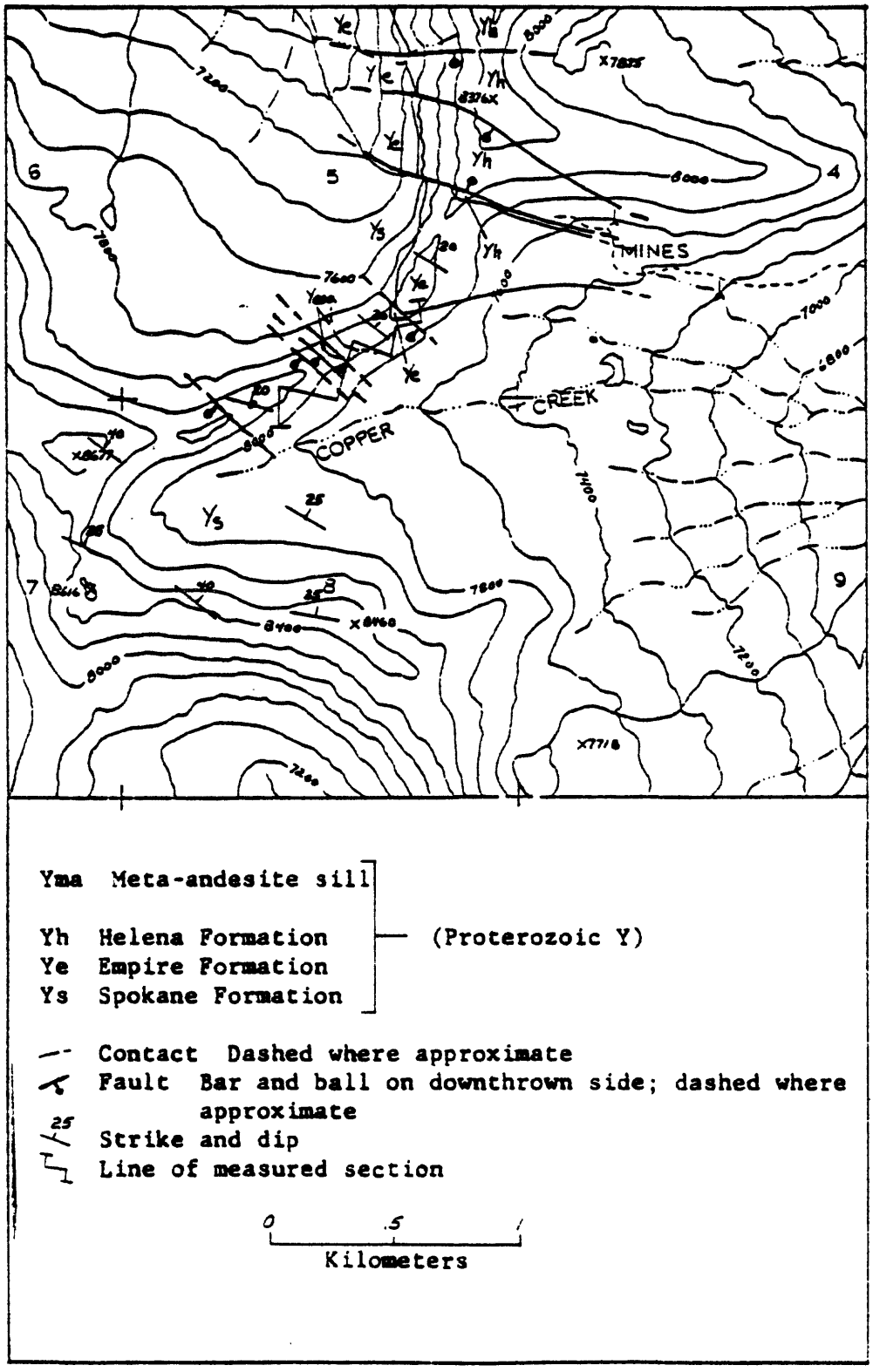

Figure 49.--Geologic map of the Copper Creek area and location of the measured section.

Empire Formation, lower part (Middle Proterozoic):	Thickness (equivalents) Meters	Feet
16. Siltite, grayish-green (5G 5/2); calcareous; platey, thin to medium lamination	0.65	2.13
15. Siltite, grayish-green; calcareous; interlaminated argillite and algal mat lamination; minor mudchip breccia and syneresis cracks	3.45	11.32
14. Quartz arenite, pale green; very fine grained; interlaminated coarse siltite	.07	.23
13. Argillite, grayish-red-purple (5RP 4/2); slightly calcareous; interlaminated siltite; limonite stringers along some bedding surfaces	1.7	5.58
12. Siltite, grayish-green; calcareous; medium to fine grained; interlaminated argillite with minor mudchip breccia	2.2	7.23
11. Siltite, grayish-green; calcareous, coarse to medium grained; interlaminated argillite, to graded rhythmites; pods and stringers of microspar as birdseye structure; oncolites, and gas expulsion pits	2.7	8.86
10. Siltite, grayish-green; calcareous; coarse to medium grained; interlaminated argillite to graded rhythmites	.85	2.79
9. Siltite, grayish-green; calcareous, coarse to medium grained; ripple laminated with argillite	1.15	3.77
8. Quartz arenite, white (N8.5); calcareous; fine grained, well sorted; rounded	.03	.1
7. Siltite; same as unit 10	2.05	6.72
6. Siltite; same as unit 9	2.8	9.18
5. Quartz arenite; same as unit 8	.1	.33
4. Siltite, grayish-green; calcareous; thin lamination	.4	1.31

Empire Formation, lower part--Continued	Thickness (equivalents) Meters	Feet
3. Siltite, pale green; slightly calcareous; blocky, thick bedding (average 53 cm); minor interbeds of very fine grained arenite	0.67	2.2
2. Siltite; same as unit 10	1.17	3.84
1. Siltite, grayish-green; calcareous; interlaminated argillite; mudchip breccia and syneresis cracks	.75	2.46
Total thickness of the Empire Formation, lower part	20.74	68.03

Spokane Formation (Middle Proterozoic) Transition zone (contact with overlying Empire Formation conformable):	Thickness (equivalents) Meters	Feet
81. Argillite, grayish-red-brown (10R 4/4); slightly calcareous; interlaminated siltite; some mudchip breccia	3.0	9.84
80. Covered	1.37	4.49
79. Siltite, grayish-red (5R 4/2); slightly calcareous; rippled laminated with very fine arenite and minor argillite	.77	2.53
78. Covered by snow	5.9	19.35
77. Argillite; same as unit 81	.75	2.46
76. Covered	2.6	8.53
75. Argillite; same as unit 81	1.9	6.23
74. Subfeldspathic arenite, reddish-purple (5RP 5/2); very fine grained; some thick bedding (30-60 cm); interbedded and interlaminated argillite; some flaser bedding	2.8	9.18
73. Siltite, grayish-green; thick lamina	.02	.07
72. Argillite; same as unit 81	3.5	11.48
71. Siltite; same as unit 73	.02	.07
70. Siltite, pale-grayish-purple (5P 5/2) to gray mottled; planar laminated with minor argillite	1.2	3.94
69. Siltite, grayish-red to tan weathering; calcareous; thin bedding	1.07	3.51
68. Argillite; same as unit 81	1.7	5.58
67. Subfeldspathic arenite, pale-green; very fine grained; thick lamina, marker	.02	.07
66. Argillite; same as unit 81	.5	1.64
65. Siltite; same as unit 69	1.9	6.23
64. Argillite, grayish-red-brown; slightly calcareous; thin lamination; some desiccation cracks	2.45	8.04

Transition zone--Continued	Thickness (equivalents) Meters	Feet
63. Siltite, pale-grayish-red (5R 5/2); calcareous; medium to fine grained	0.55	1.8
62. Siltite, grayish-red; calcareous to slightly calcareous; medium to fine grained; interlaminated argillite, some with planar lamination; mudchip breccia, desiccation cracks, and water-escape channels	10.55	34.6
61. Siltite, pale-grayish-green (5G 6/2); calcareous; thin bedding; slightly hornfelsed	.45	1.48
60. Meta-andesite, grayish-green; porphyritic; potassium feldspar; epidotized, chloritized; xenoliths of hornfelsed siltite common	3.73	12.23
59. Siltite, pale-grayish-green; calcareous; medium grained; thin bedding; some birdseye structure; slightly hornfelsed	.11	.36
58. Siltite, grayish-red; calcareous; medium grained; interlaminated argillite; desiccation cracks	1.59	5.22
57. Siltite, grayish-green; calcareous; medium grained; interlaminated argillite to graded rhythmites; birdseye structure at bottom	3.11	10.2
56. Argillite, grayish-red-brown; slightly calcareous; interlaminated siltite; desiccation cracks	.51	1.67
55. Siltite, grayish-green; calcareous; medium grained; thin bedding; birdseye structure	1.0	3.28
54. Siltite, grayish-green; calcareous; medium to fine grained; thin bedding to graded rhythmites	2.25	7.38
53. Siltite; same as unit 55	1.1	3.61
52. Siltite, grayish-green; calcareous; interlaminated argillite; syneresis cracks	.6	1.97

Transition zone--Continued		Thickness (equivalents) Meters	Feet
51.	Siltite; same as unit 54	1.35	4.43
50.	Covered	2.15	7.05
49.	Siltite; same as unit 54	.93	3.05
48.	Siltite, grayish-green; calcareous to slightly calcareous; medium to fine grained; thin bedding to graded rhythmites; stratabound chalcocite, bornite(?), and malachite	1.35	4.43
47.	Quartz arenite, grayish-green; calcareous; very fine grained; ripple laminated with coarse siltite	2.65	8.69
46.	Argillite; same as unit 56	.9	2.95
45.	Siltite, grayish-green; calcareous; coarse to medium grained; thin bedding to graded rhythmites	3.8	12.46
44.	Siltite, grayish-red; calcareous; coarse to fine grained; interlaminated argillite to graded rhythmites	1.9	6.23
43.	Siltite, grayish-red; calcareous; interbedded and interlaminated very fine grained arenite and argillite; desiccation cracks, water-escape channels, and abundant load structures	3.2	10.5
42.	Siltite, grayish-red; calcareous; interlaminated argillite as graded rhythmites, 20 mm couplets	.8	2.62
41.	Siltite, grayish-red; calcareous; interbedded and interlaminated to lenticular very fine grained arenite and argillite; desiccation cracks; grayish-green siltite marker bed (20 mm) at bottom	1.65	5.41
40.	Subfeldspathic arenite, grayish-purple (5P 4/2); calcareous; fine to very fine grained, moderately well sorted; subrounded; planar laminated; marker	.2	.7

Transition zone--Continued	Thickness (equivalents) Meters	Feet
39. Argillite, grayish-red-brown; calcareous; thinly laminated	0.4	1.31
38. Subfeldspathic arenite, grayish-purple; calcareous; fine to very fine grained, moderately well sorted; subrounded; convolute and minor ripple bedding; marker	.77	2.53
37. Subfeldspathic arenite, grayish-purple; calcareous; very fine grained; ripple to flaser bedding with argillite	.87	2.85
36. Siltite, pale-yellowish-green (10GY 7/2); coarse to medium grained; thin lamination; some mudchip breccia	.36	1.18
35. Siltite, grayish-red; slightly calcareous; interbedded very fine grained arenite and interlaminated argillite	.35	1.15
34. Argillite, grayish-red; intermittently calcareous; interlaminated siltite to graded rhythmites; one minor interbed (15 cm) of very fine grained arenite; desiccation cracks with coarse siltite fillings, and mudchip breccia common; spherical bleach marks in one 10 cm bed of coarse siltite	17.65	57.89
33. Siltite, grayish-red; calcareous to slightly calcareous; coarse to fine grained; ripple bedding with very fine grained arenite; interlaminated argillite with minor flaser bedding; desiccation cracks with very fine grained arenite fillings; white milky quartz as fracture coatings in arenites	10.97	35.98
32. Subfeldspathic arenite, grayish-red; slightly calcareous; very fine grained; thin bedding with some planar lamination, marker	1.31	4.3
31. Argillite; same as unit 56	1.05	3.44
30. Siltite, medium-greenish-gray (5G 5/1); calcareous; medium grained; medium lamination	.65	2.13

Transition zone--Continued	Thickness (equivalents) Meters	Feet
29. Siltite, grayish-red; calcareous; coarse to fine grained; interbedded fine to very fine grained arenites and argillites as graded rhythmites; rhythmic successions average 96 cm; siltites are internally graded as 25 mm couplets; arenites are ripple bedded; fine grain sized arenites are very light gray (N8), thin, moderately well sorted and rounded quartz	8.85	29.03
28. Quartz arenite, grayish-green; calcareous; very fine grained; thin bedding with coarse siltite	.18	.59
27. Siltite, medium gray (N5); calcareous; thin bedding	.97	3.18
26. Siltite, medium-greenish-gray; calcareous; interbedded fine to very fine grained rippled arenite, moderately well sorted, rounded	.9	2.95
25. Siltite; same as unit 27	2.8	9.18
24. Siltite, medium-greenish-gray; medium to fine grained; some graded rhythmites	.9	2.95
23. Subfeldspathic arenite, pale-grayish-purple (5P 5/2); calcareous; very fine grained; thick bed; load structure at base; marker	.35	1.15
22. Argillite, grayish-red-brown; slightly calcareous; thin lamination; flame structure at top of marker	.25	.82
21. Siltite, grayish-red; calcareous; medium lamination	1.07	3.51
20. Subfeldspathic arenite, pale-grayish-purple slightly calcareous; very fine grained; ripple and flaser bedding with argillite; minor interbedded siltite; load structures common	.65	2.13
19. Quartz arenite, greenish-gray to light gray (N7); calcareous; very fine grained; ripple bedding with coarse siltite	.5	.64

Transition zone--Continued	Thickness (equivalents) Meters	Feet
18. Subfeldspathic arenite; same as unit 20	2.35	7.71
17. Siltite, moderate-grayish-green (10G 5/2); calcareous; coarse to fine grained; interbedded and interlaminated with very fine grained, rippled very fine grained arenite; stratabound chalcocite, bornite(?), and malachite; one 20 cm bed of siltite containing small (2 mm) vugs filled with microspar and (or) malachite	1.25	4.1
16. Subfeldspathic arenite; same as unit 20	.7	2.3
15. Siltite, moderate-grayish-green; calcareous; medium grained; thin lamination; minor stratabound copper sulfides	1.4	4.59
14. Subfeldspathic arenite; same as unit 20	.75	2.46
13. Siltite, grayish-red; slightly calcareous; interlaminated argillite	.35	1.15
12. Siltite, moderate-grayish-green; calcareous to slightly calcareous; coarse to fine grained; thin lamination with very fine grained arenites to graded rhythmites; some moderately sorted, subrounded, rippled bedded, fine grained arenites at bottom; hackly cleavage at top; stratabound copper sulfides	1.27	4.17
11. Subfeldspathic arenite; same as unit 20	1.5	4.92
10. Siltite; moderate-grayish-green; calcareous to slightly calcareous; medium to fine grained; thin lamination with interbedded, rippled, medium to very fine grained arenite at top and bottom	.925	3.03
9. Subfeldspathic arenite; same as unit 20	1.45	4.76
8. Covered	1.3	4.26
7. Subfeldspathic arenite; same as unit 20	1.9	6.23

Transition zone--Continued	Thickness (equivalents) Meters	Feet
6. Siltite, moderate-grayish-green; calcareous to slightly calcareous; medium to fine grained; thin lamination to graded rhythmites in 3-5 mm couplets; interbedded, rippled, very fine grained arenite at base; stratabound copper sulfides	0.32	1.05
5. Subfeldspathic arenite; same as unit 20	1.3	4.26
4. Siltite; same as unit 6	.32	1.05
3. Subfeldspathic arenite, grayish-red; slightly calcareous; very fine grained; thin bedding	.47	1.54
2. Siltite; same as unit 13	.35	1.15
1. Siltite, pale-green (5G 6/2); slightly calcareous; medium grained; interbedded to interlaminated very fine grained arenite; minor stratabound copper sulfides	.27	.89
Total thickness of Transition zone	147.88	485.03

Spokane Formation, upper middle part (Middle Proterozoic):	Thickness (equivalents) Meters	Feet
38. Siltite, grayish-red; slightly calcareous; interlaminated argillite; desiccation cracks	1.2	3.94
37. Subfeldspathic arenite, pale-grayish-purple; fine to very fine grained, moderately sorted; rounded; lenticular to interlaminated with siltite	2.75	9.02
36. Subfeldspathic arenite, pale-grayish-purple; very fine grained; ripple laminated with siltite and argillite; desiccation cracks in argillite; minor 10-30 mm laminae of light-gray (N7), fine-grained quartz arenite	2.7	8.86
35. Subfeldspathic arenite, pale-grayish-purple; very fine grained; thin bedding; interbedded thinly laminated argillite in rhythmic succession	1.6	5.25
34. Siltite, grayish-red; slightly calcareous; ripple laminated with very fine grained arenite and argillite; desiccation cracks in argillite	1.85	6.07
33. Subfeldspathic arenite, pale-grayish-purple; fine to very fine grained; ripple laminated as graded rhythmites with slightly calcareous siltite and argillite; rhythmic successions average 75 cm; siltite-argillite couplets range from 10-40 mm; desiccation cracks and mudchip breccia common	2.4	7.87
32. Siltite, grayish-red; slightly calcareous; interlaminated argillite	2.25	7.38
31. Siltite, pale-green; slightly calcareous; fine grained; thick lamina	.03	.1
30. Siltite grayish-red; calcareous; medium lamination	2.2	7.22
29. Siltite; same as unit 33	1.55	5.08
28. Subfeldspathic arenite; same as unit 34	7.7	25.26
27. Siltite; same as unit 39	2.25	7.38

Spokane Formation, upper middle part--Continued	Thickness (equivalents) Meters	Feet
26. Subfeldspathic arenite, pale-grayish-purple; very fine grained; ripple laminated with slightly calcareous siltite and argillite	3.65	11.97
25. Subfeldspathic arenite, pale-grayish-purple; very fine grained; planar laminated	.35	1.15
24. Siltite, grayish-red; slightly calcareous; interbedded very fine grained arenite and interlaminated argillite	.9	2.95
23. Lithic arenite, light gray (N7); very coarse to medium grained; predominantly light-greenish-gray (5G 8/1) siltite clasts with minor clear quartz, subrounded (quartz) to well rounded clasts; thick lamina 15-25 mm	.02	.07
22. Siltite; same as unit 35	3.65	11.97
21. Subfeldspathic arenite, pale-grayish-purple to light gray; slightly calcareous; fine to very fine grained; distinguished by spherical bleach marks, average 55 mm diameter	.05	.16
20. Siltite, grayish-red; fine grained; interlaminated argillite; desiccation cracks and mudchip breccia	3.3	10.82
19. Subfeldspathic arenite, pale-grayish-purple; very fine grained; very thick bed; marker; characterized by milky quartz veins and fracture coatings	1.12	3.67
18. Siltite; same as unit 35	5.05	16.56
17. Subfeldspathic arenite, pale-grayish-purple; very fine grained; thin bedding; ball-and-pillow structure at base	1.35	4.43
16. Siltite, grayish-red; coarse grained; interlaminated very fine grained quartz arenite	1.55	5.08
15. Subfeldspathic arenite; same as unit 26	.45	1.48

Spokane Formation, upper middle part--Continued	Thickness (equivalents) Meters	Feet
14. Siltite, light-pale-green (10G 7/2); coarse to medium grained; thin planar lamination at base to interbedded with very fine grained arenite at top	1.01	3.31
13. Siltite, grayish-red; coarse grained; minor interbeds of very fine grained arenite, some tangential crossbedding	2.65	8.69
12. Siltite, grayish-red; coarse to fine grained; interlaminated moderate-reddish-brown (10R 4/4) argillite; minor interlaminated, lenticular very fine grained arenite; desiccation cracks and water-escape channels in argillite filled with coarse siltite; mudchip breccia and spherical bleach marks	7.95	26.08
11. Subfeldspathic arenite, pale-grayish-purple; thin bedding; chlorite coatings on fractures	.6	1.97
10. Siltite; same as unit 13	1.0	3.28
9. Siltite; same as unit 17	4.35	14.27
8. Subfeldspathic arenite; same as unit 18	.35	1.15
7. Siltite, grayish red; coarse grained; interbedded and interlaminated very fine grained arenite and argillite	3.35	10.99
6. Subfeldspathic arenite; same as unit 36	1.75	5.74
5. Siltite, grayish-red; fine grained; interlaminated argillite; hackly cleavage	.75	2.46
4. Siltite; grayish-red; coarse grained; thin bedding with minor very fine grained arenite and argillite, some ripple bedding	1.75	5.74
3. Quartz arenite, medium gray (N5); fine grained, well sorted; subrounded; thick, rippled lamina	.03	.1

Spokane Formation, upper middle part--Continued	Thickness (equivalents) Meters	Feet
2. Siltite, grayish-red; coarse to fine grained; interbedded and interlaminated very fine grained arenite and argillite to graded rhythmites; desiccation cracks in argillite	4.8	15.74
1. Subfeldspathic arenite; pale-grayish-purple; very fine grained; thin to medium bedding (6-26 cm); interbedded fine grained siltite; load structures	1.7	5.58
Partial thickness of upper middle Spokane Formation	81.96	268.83

Diamond Drill Holes

During the summer seasons of 1963 and 1964, Bear Creek Mining Company drilled several holes into the Spokane Formation in search of favorable stratabound copper-silver occurrences. Three of their holes are of interest in this study as two are collared in the lower Empire Formation and all penetrated the transition zone and some depth beyond. Drill logs prepared by Bear Creek geologists are reconstructed in this report and used with the permission of the Company.

All the holes are located near Lincoln, Montana, progressively east to southeast of each other and the measured sections (fig. 1). Holes A-3 and A-5 are located in the Alice Creek drainage on flanking ridge tops. Drill hole CH-2 is southeast of the Heddleston Mining district on a ridge top near the headwaters of Canyon Creek. Old drill roads presently provide access by jeep to the drill sites.

Drill holes A-3 and A-5 are located very near the axis of a gentle syncline. Small, local shear zones were encountered by the holes, but displacement was small based on surface geology and thickness of gouge zones. Hole CH-2 lies northeast of a major northwest-trending normal fault; however, the fault dips to the south and does not interrupt the stratigraphic section. Thin meta-andesite sills of apparent Proterozoic age, similar to the one at Copper Creek, intrude the transition zone in hole CH-2. Two sills, the upper 1.9 m thick and the lower 0.7 m thick, are separated by a red bed 0.7 m thick. Effects of contact metamorphism are not noted in the log and are apparently negligible. There is no reason based on surface geology and drill logs to suspect that any of the three drill holes are faulted as extensively as the Copper Creek section.

All measurements on drill logs are in feet, converted to meters for the purpose of this study. Drill logs were reconstructed to stratigraphic logs where description of core permitted. As noted previously, selection of the boundary between the Empire Formation and the Spokane Formation was made differently by Bear Creek geologists than is currently practiced. Core from the three holes is not available for study as it has been disposed of or only a skeleton core remains.

The following discussion of each hole summarizes the subdivision of units and their respective thicknesses and lithologies.

A-3--Of the three holes, A-3 has the best stratigraphic control and log. Total depth of the hole is 315.85 m. Subdivision of the section based on criteria used for the measured sections results in 32.16 m of Ye, 81.29 m of transition zone, and 90.1 m of upper middle Ys. The 90.1 m of upper middle Ys is not the total remaining drill log but rather the upper portion used for comparative purposes.

Lower Empire strata are characterized by pale greenish siltites and minor interlaminated argillites. These units often display a tan weathering coloration, especially along fractures, due to a high carbonate content. Near the base of the Empire are two units of red argillite with interlaminated siltite.

Siltite interlaminated with argillite appears to dominate the transition zone. Minor quartz arenite units are present, especially in green and gray sequences. Small-scale "crossbedding" is noted in both red and green strata. Two distinct intervals of green bed units are easily identified. The upper interval is 16 m thick; however, brecciation and alteration of the lower part indicates faulting and possible thickening of the interval. The lower interval is separated by red beds from the upper one and consists of 9 green units alternating with red beds. This interval spans a thickness of 29.4 m, of which the lowermost green unit forms the base of the transition zone.

Below the transition zone, there is a distinct increase in the number of red to pink arenites interbedded with gray to red "coarse" siltites. Interlamination of argillite is still noted, and, likewise, green bands or layers less than 5 cm thick are frequently present, decreasing downward and absent 50 m below the top. Small-scale "crossbedding" is common in most units.

No mention of carbonate content is made in this hole except the description of numerous calcite and quartz-calcite veins crosscutting the core. The presence of tan "alteration" is likely the result of carbonate cements in the rock as is found in the McCabe and Copper Creek sections.

A-5--Located some 4.8 km southwest of A-3, A-5 is collared very near the Ye-transition zone contact, based on surface geologic mapping. Consequently, no Empire was cored. Subdivision of the section results in 67.69 m of exposed transition zone and 31.22 m of upper middle Ys, which is included in this discussion. Total depth of section penetrated is approximately 305 m.

Transition zone strata are mostly siltites with interlaminated argillites often as graded beds. Red argillite is dominant over siltite at the top of the zone and contains scattered bands of green argillite less than 15 cm. Thin interbeds of arenite are present in green units, but generally less in number than A-3. Once again, two distinct green intervals are present. Figure 41 adequately illustrates these intervals and their stratigraphic positions.

The upper portion of the lower subdivision (upper middle Ys) is dominated by siltite with argillite and thin interbeds of green siltite less than 10 cm. Red and gray arenite dominate most of the remaining part (lower 14.3 m) and clearly are in greater abundance as individual sedimentation units than found elsewhere upsection.

CH-2--Further southwest from A-3, 13.5 km along the regional strike, hole CH-2 is collared in lower Empire strata and penetrates a depth of approximately 400 m. The stratigraphic control recorded on the log of CH-2 is much less precise than that of A-3 or A-5, such that complete subdivision of the section is difficult at best. No difficulty is experienced in defining the upper boundary of the transition zone or Ye/Ys contact, but the lower boundary of the transition zone is another matter. Based on descriptions of carbonate content and grain size of lithology, selection of the lower transition zone boundary resulted in a thickness of 160 m of TZ. This decision left 44.9 m of Ye at the top of the section and 69.4 m of the upper middle Ys were designated as the lower subdivision.

As interpreted from the log, the lower Empire is dominated by green to yellow argillite, some of which is "limonitic". At the base of this subdivision and immediately above the Ye/Ys contact, the Empire is dominated by coarser siltite. All the units are calcareous.

The transition zone is composed of the usual mixture of siltite and argillite with little mention of arenite. Especially noteworthy is the apparent absence of two green intervals within the subdivision. The upper thicker interval is present, but no distinct mention is made of the alternating green and red interval at the base. The log does describe ". . . thin gray or green gray. . . interbeds. . ." which occur 57 m above the base of the transition zone and are present upsection for an unkncwn distance. This could be the lower green interval. Carbonate content decreases downward in the zone and is described as slightly calcareous at the bottom (note: this vertical distribution is artificial since the lower boundary of the TZ was partly selected using carbonate content). Two meta-andesite sills intrude the zone below the upper green interval. These sills closely resemble the one in the Copper Creek section and those described by Earhart (1975) as Proterozoic.

Below the TZ, carbonate was not recorded, grain size coarsens in siltites, arenite is more prevalent, and beds become thicker and more massive. These trends were all observed in the other sections, and thus the selected subdivision boundaries seem relatively consistent.